UCRL-TR-232463

LAWRENCE
LIVERMORE
NATIONAL
LABORATORY

Survey of Materials for Fusion Fission Hybrid Reactors Vol 1 Rev. 0

J.C. Farmer

July 3, 2007

Disclaimer

This work performed under the auspices of the U.S. Department of Energy by Lawrence Livermore National Laboratory under Contract DE-AC52-07NA27344.

UCRL-TR-232463

Survey of Materials for Fusion Fission Hybrid Reactors

Volume 1

Joseph Collin Farmer
Chemistry Materials and Life Sciences Directorate
Lawrence Livermore National Laboratory
7000 East Avenue
Livermore, California 94550

July 4th 2007

Executive Summary

Materials for fusion-fission hybrid reactors fall into several broad categories, including fuels, blanket and coolant materials, cladding, structural materials, shielding, and in the specific case of inertial-confinement fusion systems, laser and optical materials. This report surveys materials in all categories of materials except for those required for lasers and optics.

Preferred collants include two molten salt mixtures known as FLIBE (Li_2BeF_4) and FLINABE ($LiNaBeF_4$). In the case of homogenous liquid fuels, UF_4 can be dissolved in these molten salt mixtures. The transmutation of lithium in this coolant produces very corrosive hydrofluoric acid species (HF and TF), which can rapidly degrade structural materials.

Broad ranges of high-melting radiation-tolerant structural material have been proposed for fusion-fission reactor structures. These include a wide variety of steels and refractory alloys. Ferritic steels with oxide-dispersion strengthening and graphite have been given particular attention. Refractory metals are found in Groups IVB and VB of the periodic table, and include Nb, Ta, Cr, Mo, and W, as serve as the basis of refractory alloys. Stable high-melting composites and amorphous metals may also be useful. Since amorphous metals have no lattice structure, neutron bombardment cannot dislodge atoms from lattice sites, and the materials would be immune from this specific mode of degradation.

The free energy of formation of fluorides of the alloying elements found in steels and refractory alloys can be used to determine the relative stability of these materials in molten salts. The reduction of lithium transmutation products (H^+ and T^+) drives the electrochemical corrosion process, and liberates aggressive fluoride ions that pair with ions formed from dissolved structural materials. Corrosion can be suppressed through the use of metallic Be and Li, though the molten salt becomes laden with colloidal suspensions of Be and Li corrosion products in the process. Alternatively, imposed currents and other high-temperature cathodic protection systems are envisioned for protection of the structural materials. This novel concept could prove to be enabling technology for such high-temperature molten-salt reactors.

The use of UF_4 as a liquid-phase homogenous fuel is also complicated by redox control. For example, the oxidation of tetravalent uranium to hexavalent uranium could result in the formation of volatile UF_6. This too could be controlled through electrochemically manipulated oxidation and reduction reactions.

In situ studies of pertinent electrochemical reactions in the molten salts are proposed, and are relevant to both the corrosive attack of structural materials, as well as the volatilization of fuel.

Some consideration is given to the potential advantages of gravity fed falling-film blankets. Such systems may be easier to control than vortex systems, but would require that cylindrical reaction vessels be oriented with the centerline normal to the gravitational field.

Introduction

Materials for fusion-fission hybrid reactors fall into several broad categories, including fuels, blanket and coolant materials, cladding, structural materials, shielding, and in the specific case of inertial-confinement fusion systems, laser and optical materials. The following categories of materials for fusion-fission hybrid reactors are discussed, with the exception of laser and optical materials.

- Fuels
- Blanket & Coolant
- Neutron Multiplier
- Cladding
- Structural
- Shielding
- Laser & Optical

The information discussed within this report was obtained from searches of the published scientific and technical literature, as well as searches of published United States patents pertaining to first-wall materials for fusion reactors. These searches are summarized in Appendices A and B. This report will be revised and updated in the future to provide additional information.

Preferred collants include two molten salt mixtures known as FLIBE (Li2BeF4) and FLINABE (LiNaBeF4). In the case of homogenous liquid fuels, UF_4 can be dissolved in these molten salt mixtures. The transmutation of lithium in this coolant produces very corrosive hydrofluoric acid species (HF and TF), which can rapidly degrade structural materials.

Broad ranges of high-melting radiation-tolerant structural material have been proposed for fusion-fission reactor structures. These include a wide variety of steels and refractory alloys. Ferritic steels with oxide-dispersion strengthening and graphite have been given particular attention. Refractory metals are found in Groups IVB and VB of the periodic table, and include Nb, Ta, Cr, Mo, and W, as serve as the basis of refractory alloys. Stable high-melting composites and amorphous metals may also be useful. Since amorphous metals have no lattice structure, neutron bombardment cannot dislodge atoms from lattice sites, and the materials would be immune from this specific mode of degradation.

The free energy of formation of fluorides of the alloying elements found in steels and refractory alloys can be used to determine the relative stability of these materials in molten salts. The reduction of lithium transmutation products (H^+ and T^+) drives the electrochemical corrosion process, and liberates aggressive fluoride ions that pair with ions formed from dissolved structural materials. Corrosion can be suppressed through the use of metallic Be and Li, though the molten salt becomes laden with colloidal suspensions of Be and Li corrosion products in the process. Alternatively, imposed currents and other high-temperature cathodic protection systems are envisioned for protection of the structural materials. This novel concept could prove to be enabling technology for such high-temperature molten-salt reactors.

The use of UF_4 as a liquid-phase homogenous fuel is also complicated by redox control. For example, the oxidation of tetravalent uranium to hexavalent uranium could result in the formation of volatile UF_6. This too could be controlled through electrochemically manipulated oxidation and reduction reactions.

In situ studies of pertinent electrochemical reactions in the molten salts are proposed, and are relevant to both the corrosive attack of structural materials, as well as the volatilization of fuel.

Some consideration is given to the potential advantages of gravity fed falling-film blankets. Such systems may be easier to control than vortex systems, but would require that cylindrical reaction vessels be oriented with the centerline normal to the gravitational field.

Fuels

Several forms of fissile materials can be considered tin the design of a fusion-fission hybrid reactor. These include uranium and a wide variety of uranium compounds. Many of these high melting point compounds, such as UO2, are suitable for solid-phase fuel elements. Some key attributes of these fuels are summarized in Table 1, and are listed from the highest to the lowest melting point.

Table 1. Density and Melting Points of Candidate Fissionable Fuels

Uranium Compound	Density (g/cm^3)	Melting Point (°C)	Analog	Structure
UN	14.32	2850	NaCl	Cubic
UO_2	10.97	2880	CaF_2	Cubic
UC_2	11.68	2470		Tetragonal
UC	13.63	2370	NaCl	Cubic
USi	10.40	1600		Orthorhombic
UAl_2	8.10	1590		
UAl_3	6.70	1320		
U	19.13	1133		
Th_4	6.32	1114		
UF_4	6.70	1036		
UAl_4	6.00	730		

Compounds such as UF_4 and Th_4 are soluble in molten salts comprised of lithium fluoride and beryllium fluoride, such as FLIBE [Ursu, Chapter 7, p. 247, 1985]. These dissolved uranium and thorium salts can therefore be used as homogenous liquid phase fuels. Unfortunately, if these materials become oxidized, with the oxidation state increasing, problematic volatile compounds can form. The gaseous UF6 species is very well known, and could form during the inadvertent oxidation of UF_4. Such volatilization could be controlled through electrochemical control and manipulation of the uranium oxidation state.

Concepts for blanket/coolant materials have evolved over several decades. That evolution is discussed in the book by Ursu [1985], as well as in earlier articles by Grimes and Cantor [1972] and others. The early evolution of these concepts is briefly summarized as follows:

- 1957 (UKAEA, Harwell)
    - $^{238}U - {}^{6}Li$
- 1957 (KAPL)
    - UO_2SO_4
- 1965 (MIT)
    - $LiF - BeF_2 - UF_4$
    - $LiF - UF_4$
- 1969 (MIT)
    - $71\%LiF - 2\%BeF_2 - 27\%ThF_4$
- 1970 (MIT)
    - $^{235}U - {}^{233}U - {}^{239}Pu - {}^{6}Li$
- 1972 (PNL)
    - Natural Uranium
- 1972 (ORNL) [Grimes et al. 1972]
    - FLIBE: Li_2BeF_4
    - FLINABE: $LiNaBeF_4$

Blanket/Coolant Materials

At the present time, two competing concepts exist for liquid blanket/coolant, protecting the structural first-wall of fusion and fusion-fission hybrid reactors: (1) liquid lithium; and (2) molten lithium-beryllium fluoride salts:

- Liquid Metals Previously Considered
    - Hg, Na, K, Pb, Bi, Pb-Bi, Sn, Li, Li-Al, Pb-Li, Sn-Li, etc.
- Natural Li is 92.58% ^{7}Li and 7.42% ^{6}Li
    - Absorption cross-section for thermal neturons
    - Natural Lithium ~ 70b
    - ^{7}Li ~ 0.033b
- Molten Salts Previously Considered
    - FLIBE Blanket/Coolant: $2LiF + BeF_2 = Li_2BeF_4$
    - Uranium/Thorium Fluoride Solution: Li_2BeF_4 Variants with UF_4 and Th_4
    - FLINABE Blanket/Coolant: $LiF + NaF + BeF_2 = LiNaBeF_4$
    - Uranium/Thorium Fluoride Solution: $LiNaBeF_4$ Variants with UF_4 and Th_4
    - $^{24}NaBF_4 + {}^{24}NaF$ (Secondary / Intermediary)

Molten salts have been considered as coolants for graphite-moderated molten-salt breeder reactors that operate on the thorium-uranium fuel cycle with continuous reprocessing of the fuel. Reprocessing is used to keep fission products at desirable levels.

FLIBE melts at relatively high temperature. The salt mixtures corresponding to the eutectic composition has a melting point greater than 600K. Pure FLIBE has relatively low viscosity, comparable to kerosene at ambient temperature, and therefore would be expected to flow well. It is said to have good compatibility with graphite and various nickel-based alloys, though more recent papers have begun to document corrosion problems associated with the formation of corrosive HF and TF during transmutation of lithium.

As discussed by Petti et al. [2006], the second Japan/US Program on Irradiation Test for Fusion Research (Jupiter-II) began on April 1, 2001. Part of the collaborative research has centered on studies of molten Li_2BeF_4, which is also known as FLIBE.

Table 1 – Blanket and Coolant Properties

	MW	Density (kg/m^3)	MP (°C)	BP (°C)
Li	6.939	554	179	1317
Be	9.0122	1820	1283	2970
Na	22.989	970	97.81	892
K	39.102	860	63.65	774
LiF	25.94	2300	842	1676
BeF_2	47.01	1086	Sublimes at 800	Sublimes at 800

In cases where the molten salt is used to dissolve UF4 to form a homogeneous liquid fuel system, it is unknown whether or not the corrosive effects of pure lithium fluoride ($LiF+UF_4$) are better or worse than that of FLIBE (Li_2BeF_4 + UF_4). However, in the case of pure FLIBE, the introduction of metallic beryllium (Be) into FLIBE is considered a viable means of mitigating corrosion, since it promotes the conversion of hydrofluoric acid species to hydrogen (HF/TF to H_2/HT). Unfortunately, this approach to corrosion control not without a liability, since the beryllium forms a "grey solution" due to what may be the suspension of colloidal beryllium, which may have to be removed during “salt cleanup”.

Tritium Release from FLIBE

In regard to the tritium release behavior of FLIBE, these investigators heated 100 to 300 grams of FLIBE to a temperature of 873K in a Monel crucible placed in a fast-neutron reactor, which was located at the University of Tokyo (YAYOI). The neutron flux during these irradiations was 10^8 to 10^9 n cm^{-2} sec. At hydrogen partial pressures above 1000 Pa, the primary tritium-bearing species responsible for tritium release is gaseous diatomic HT. Nishimura et al. [2001] provide the normalized release rates for tritium in flowing stream of helium purge gas with various concentrations of hydrogen. The normalized tritium release rate drops dramatically below hydrogen partial pressures of 1000 Pa. Steady state was achieved after approximately 120 to 140 minutes of purging.

However, thermal neutrons from the reactor react with Li^+ and convert this alkali metal ion to T^+, which react with fluoride anions in the melt to form gaseous TF, which is chemically similar to hydrogen fluoride). The tritons (T^+) in the molten salt electrolyte also participate in exchange reactions with gaseous diatomic hydrogen (H_2) to form HT and protons (H+). Clearly, the tritium release behavior from the FLIBE will be controlled by the oxidation-reduction reactions in the electrolyte. In fact, it is conceivable that on-line electrolytic cells could be used to promote and control tritium release from the electrolyte, which would provide substantial advantages in controlling the overall process.

Neutron Multipliers

Current fusion reactor concepts consider the application of beryllium as neutron moderator and neutron multiplier [Ursu 1985, Section 12.5.3, p. 434]. With the advent of fusion and fusion-fission reactors in the future, beryllium is expected to become and increasingly important material. Published estimates indicate that a fusion reactor generation capacity of one-million megawatts will require approximately 4.6×10^7 kilograms of beryllium. Beryllium is a light metal with an elastic modulus slightly superior to that of steel, and does not readily oxidize in air. However, beryllium and its salts, including FLIBE and FLINABE are considered very toxic and will have to be handled very carefully. Assuming an eight-hour work day, the maximum allowable concentration of beryllium aerosol in a fusion reactor facility should be no more than 2 micrograms per cubic meter. Exposure of he public should be no more than 0.01 micrograms per cubic meter.

Structural Materials

There are several broad categories of high-temperature materials from which materials can be selected for the construction of fusion-fission hybrid reactors. These broad categories and the temperature level bounding the upper operating temperature for each, is summarized below:

- Refractory Metals < 4000°C
- Carbides < 4000°C
- Nitrides < 3500°C
- Borides < 3500°C
- Oxides < 3000°C
- Intermetallics < 3000°C
- Silicides < 2500°C
- Sulfides < 2500°C
- Steels < 670°C

Zinkle et al. have performed and outstanding critical analysis of the operating temperature windows for nine candidate structural materials for fusion reactors [Zinkle et al. 2004]. These include: four reduced-activation structural materials (oxide-dispersion-strengthened and ferritic/martensitic steels containing 8-12%Cr, V-4Cr-4Ti, and SiC/SiC composites), copper-base alloys (CuNiBe), tantalum-base alloys (e.g. Ta-8W-2Hf), niobium alloys (99Nb-1Zr), and molybdenum and tungsten alloys. The results are compared with the operating temperature limits for Type 316 austenitic stainless steel. Several factors define the allowable operating temperature window for structural alloys in a fusion reactor. The lower operating temperature limit in all body-centered cubic (bcc) and most face-centered cubic (fcc) alloys is determined by radiation embrittlement (decrease in fracture toughness), which is generally most pronounced for irradiation temperatures below similar to 0.3 T-M where T-M is the melting temperature. The lower operating temperature limit for SiC/SiC composites will likely be determined by radiation-induced thermal conductivity degradation, which becomes more pronounced in ceramics with decreasing temperature. The upper operating temperature limit of structural materials is determined by one of four factors, all of which become more pronounced with increasing exposure time: (1) thermal creep (grain boundary sliding or matrix-diffusion creep); (2) high temperature He embrittlement of grain boundaries; (3) cavity swelling (particularly important for SiC and Cu alloys); or (4) coolant compatibility/corrosion issues. In many cases, the upper temperature limit will be determined by coolant corrosion/compatibility rather than by thermal creep or radiation effects.

Refractory Metals and Alloys for First-Wall Applications

Refractory alloys are of particular interest for fusion and fusion-fission hybrid reactors due to: relatively high melting points, which enable this type of material to maintain high strength at elevated temperature. Refractory alloys are much more formable than ceramics.

Refractory metals are found in Groups IVB, VB and VIB of the periodic table, and include Nb, Ta, Cr, Mo, and W. Specifically, these materials include:

- Carbon: AW 12.011, AN 6, MP 3367°C, SUB 3367±25°C, BP 4827°C
    - Amorphous : $\rho = 1.8$ to 2.1 g/cm^3 (25°C)
    - Graphite: $\rho = 1.9$ to 2.3 g/cm^3 (25°C)
    - Diamond: 3.15 to 3.5 g/cm^3 (25°C)
    - Notes. The favorable high-temperature properties of graphite have led to its prolific use in aerospace applications. The graphitic form consists of parallel planes of carbon atoms, arranged in hexagonal cells. This unique structure enables graphite to form intercalation compounds with lithium cations (Li+). The tendency of graphite to from intercalation compounds with the lithium cations in FLIBE and FLINABE would prove problematic in a fusion-fission hybrid reactor. This well-known characteristic has led to the use of graphite as the preferred cathode material in virtually all modern high-performance rechargeable Li-ion batteries.
- Tungsten: AW 183.85, AN 74, MP 3410±20°C, BP 5660°C, $\rho = 19.3$ g/cm^3 (20°C)
    - Ores: wolframite [$(Fe,Mn)WO_4$], scheelite [$CaWO_4$], huebnerite [$MnWO_4$], ferberite [$FeWO_4$]
    - Sources: California, Colorado, South Korea, China, Bolivia, Ukraine/Russia
    - Notes. Tungsten is also known as Wolfram. It is a true metal with the highest melting point and lowest vapor pressure; tantalum-carbide/graphite composite melts at 6760 °C. It forms oxides that are relatively insoluble in acid, and is one of the alloying elements added to austenitic nickel-chromium-molybdenum alloys to stabilize passive film in acidic oxidizing regions of the Pourbaix diagram, and significantly increases the pitting resistance equivalence number (PREN) of these alloys. In regard to the current nuclear fuel cycle, it is a key ingredient of nickel-based Alloy C-22 that will be used to construct 11,000 disposal containers for the Nation's 70,000 MTU spent nuclear fuel.

- Tantalum: AW 180.95, AN 73, MP 2996°C, BP 5424±100°C, $\rho = 16.654$ g/cm^3 (20°C)
    - Ores: columbinte-tantalite [$(Fe,Mn)(Mn,Ta)_2)_6$]
    - Sources: Zaire, Brazil, Mozambique, Thailand, Portugal, Nigeria, Canada
- Molybdenum: AW 95.94, AN 42, MP 2617°C, BP 4612°C, $\rho = 10.22$ g/cm^3 (20°C)
    - Ores: molybdenite [MoS_2], wulfenite [$(PbMoO_4)_3$], powellite [$Ca(Mo,W)O_4$]
    - Sources: relatively plentiful
    - Note: This material is a byproduct of copper and tungsten mining; many ultra-high strength steels with yield strengths above 300,000 pounds per square inch (psi) contain this element at 0.25 to 8 weight percent. This alloying element is also added to austenitic stainless steels and nickel-chromium-molybdenum alloys (Type 316L Stainless, Hastelloys^{TM} and Inconels^{TM}) to stabilize passive film in acidic oxidizing regions of the Pourbaix diagram, and significantly increases the pitting resistance equivalence number (PREN) of these materials. Even more important than tungsten in regard to its role in high-performance nickel-based alloys, it is a key ingredient of nickel-based Alloy C-22. In regard to the current nuclear fuel cycle, high-molybdenum Alloy C-22 will be used to construct 11,000 disposal containers for the Nation's 70,000 MTU spent nuclear fuel; sulfide serves as solid lubricant; catalyst; essential trace element for plant nutrition. Due to the entry of the Chinese into the world metals market, the costs of such high-performance alloys have skyrocketed. Recent procurements of Alloy C-22 were at a cost of $37 per pound, driven significantly by the cost of both nickel and molybdenum.
- Niobium: AW 92.91, AN 41, MP 2468±10°C, BP 4742°C, $\rho = 8.57$ g/cm^3 (20°C)
    - Ores: associated with carbonatities; niobite-tantilite; pyrochlore; euxenite
    - Sources: Canada, Brazil, Nigeria, Zaire, Ukraine/Russia
    - Notes. Niobium is also known as Columbium, and is unique in that it has superconductive properties.

- Vanadium: AW 50.94, AN 23, MP 1890±10°C, BP 3380°C, $\rho = 6.11$ g/cm^3 (18.7°C)
    - Ores: carnotite, roscoelite, vanadinite, patronite
    - Sources: relatively plentiful
    - Notes. Vanadium forms refractory alloys that have been shown to have reasonably good corrosion properties in the presence of liquid lithium, FLIBE and FLINABE. This element is plentiful, and is found in over 65 different minerals. Its ores are frequently associated with phosphate rock and iron ore.
- Chromium: AW 51.996, AN 24, MP 1857±20°C, BP 2672°C, $\rho = 7.18$ g/cm^3 (20°C)
    - Ores: chromite [$FeCr_2O_4$]
    - Sources: Southern Rhodesia, Russia/Ukraine, Turkey, Iran, Albania, Finland, Madagascar, Philippines
    - Note: Chromium is produced through the chemical reduction of oxide ore with metallic aluminum, which is produced electrolytically. From an environmental point of view, chromium is paradoxical: hexavalent chromium is carcinogenic, while trivalent chromium is essential for human life. Chromium is the element primarily responsible for passive film formation on iron-based 300-series stainless steels, including Types 304L and 304L. The passive film formed from chromium is stable over modest ranges of potential and pH. Due to its role in the passivity of steels, it is also a key ingredient of nickel-based Alloy C-22. As previously discussed in regard to tungsten and molybdenum, Alloy C-22 will be used to construct 11,000 disposal containers for the Nation’s 70,000 MTU spent nuclear fuel.
- Platinum: AW 195.09, AN 78, MP 1772°C, BP 3827±100°C, $\rho = 21.45$ g/cm^3 (20°C)
    - Ores: metal [native form]; sperrylite [$PtAs_2$]
    - Sources: Colombia, Canada, Western United States, Others
    - Note. Platinum occurs in native form as silvery-white metal, and usually found with lesser amounts of iridium, osmium, palladium, ruthenium, and rhodium. This white precious metal recognized by pre-Colombian men in the Americas. Platinum is unique in its outstanding catalytic and electrocatalytic properties, and is the catalyst of choice in proton exchange membrane fuel cells for both oxygen cathodes and hydrogen anodes, at loadings of 0.5 to 2.0 mg/cm^2. As the world moves towards a hydrogen economy, the demands and costs are likely to rise significantly, until alternative electrocatalysts are created through bandgap engineering.

- Titanium: AW 47.90, AN 22, MP 1660±10°C, BP 3287°C, $\rho = 4.54$ g/cm^3 (20°C)
  - Ores: rutile, ilmenite, sphene
  - Sources: relatively plentiful
  - Notes. The National Strategic Reserve of Titanium Metal is located in Henderson, Nevada, at TIMET, Incorporated. At the present time, the Department of Defense is investing heavily in processes to achieve dramatic reductions in the cost of titanium, by shifting from chemical to electrolytic reduction, as was done for aluminum production in the early 20th century. It is frequently alloyed with small amounts of palladium to enhance its environmental resistance. Approximately 12.1 weight percent of Moon Rocks collected during Apollo 17 mission consisted of rutile (TiO_2), and most white paint pigment consists of rutile, which was used as a safe alternative to lead oxide. This particular oxide has unique photocatalytic properties. Titanium is strong lightweight metal used for many aerospace and defense applications. It is extremely corrosion resistant in saline environments, and is one of the materials of choice in desalination plants. In regard to the current nuclear fuel cycle, more than 10,000 titanium alloy (Ti Grade 7) drip shields are planned for emplacement in Yucca Mountain to protect waste packages from rock drop and dripping ground water, and will cost several billion dollars.

Several refractory alloys have been explored for possible application as first-wall materials in fusion reactors [Ursu 1985; patent literature]. Several specific alloy compositions are given below.

- Molybdenum Alloys
  - 99.4%Mo-0.5%Ti-0.08%Zr-0.01%C
  - 93%Mo-7at.%Re to 70%Mo-30at.%Re
- Niobium Alloys
  - 81%Nb-10%Mo-3%Ti-1%Zr
- Vanadium Alloys
  - 80%V-20%Ti
  - (81-94)%V-(3-9)%Cr-(3-10)%Ti
  - V-4Cr-4Ti

Tungsten Alloys

United States Patent 7,128,980 [Appendix A] discloses a novel tungsten-based composite for first-wall applications in fusion reactors. A layer of tungsten-based alloys is used to face the high-temperature plasma, exploiting its high-temperature refractory properties, while copper alloys are used to enhance heat transfer. Specifically, this laminated composite consists of a plasma-facing area made of tungsten or a tungsten-based alloy (tungsten concentration greater than 90 weight %) and a heat-dissipating area made of copper or a copper-based alloy, with a thermal conductivity of at least 250 W/m-K, a mean grain size of greater than 100 microns.

The regions separating the heat-resistant tungsten-alloy face and the heat-dissipating copper face is separated by a refractory-metal-copper composite; the refractory-metal-copper composite having a macroscopically uniform copper and tungsten concentration progression and a refractory metal concentration ranging from 10 to 40 volume % throughout material’s thickness of 0.1 mm to 4 mm. The refractory metal phase forms a virtually continuous skeleton in this composite structure. Refractory-metal-copper composites with nearly continuous skeletons can also be produced by pressing powder mixtures or composite powders and sintering. Aside from W-Cu and Mo-Cu composites produced in this way, the use of rolled or extruded Mo-Cu composites has proven to be particularly advantageous.

Suitable tungsten materials for the plasma-facing segment include monocrystalline tungsten, pure tungsten, AKS (aluminum-potassium-silicate doped) tungsten, UHP (ultra-high-purity) tungsten, nanocrystalline tungsten, amorphous tungsten, ODS (oxide-dispersion-strengthened) tungsten, W-Re, ODS-W-Re and carbide-, nitride, or boride-precipitation-hardened tungsten alloys with preferred a carbide, nitride or boride concentration of between 0.05 and 1 vol. %. Segmentation of the tungsten/tungsten-alloy components is advantageous. As the crack propagation rate of the tungsten components is significantly higher in the direction of deformation than perpendicular to it, it may be advisable in the case of parts exposed to high levels of stress to produce the tungsten parts in such a way that the direction of deformation is perpendicular to the plasma-facing surface.

In order to achieve sufficient structural stability and rigidity, a component consisting of a metallic material with a strength of more than 300 MPa is bonded to the copper segment. Particularly suitable metallic materials include age-hardened Cu--Cr--Zr, and ODS-Cu materials as well as austenitic steels.

Molybdenum Alloys

Molybdenum alloy with small additions of titanium, zirconium and carbon, such as 99.4%Mo-0.5%Ti-0.08%Zr-0.01%C, have good strain endurance and fracture toughness at high temperature. However, their susceptibility to oxidation requires that it be coated with thermal-spray coatings of Si-Al-Co. Other cladding is also possible. Additions of rhenium have been used to improve the ductility and fabricability of molybdenum alloys. Specific Re-containing molybdenum alloys that have been developed include: Mo-7Re (13 wt. % Re); Mo-27Re (42 wt. % Re); and Mo-30Re (45 wt. % Re). After neutron irradiation of Mo-27Re and Mo-30Re at 750 to 1075°C, $MoRe_3$ (Chi phase) precipitates formed at grain boundaries and on the surface at a damage level of 1.5 dpa; these precipitates were not observed in Mo-7Re [Ursu 1985].

Niobium Alloys

These materials also have good strain endurance and fracture toughness. Some of the best tensile properties obtained with niobium-based alloys have been reported with: (1) Nb-15%W-3%Ti-1%Zr and (2) Nb-10%-3%Ti-1%Zr. Titanium additions have enhanced the hardness of these alloys, and have improved their refractory properties, allowing them to operate at temperatures as high as 1300°C. These materials tend to have better ductility than Mo alloys. Furthmore, these materials can be prepared using cold and hot pressing. Furthermore, argon arc welding is possible. Coatings of silicon have been used to prevent high temperature oxidation [Ursu 1985].

Vanadium Alloys for First-Wall Applications

Vanadium alloys for fusion first-wall/blanket structural applications have been investigated by Smith et al. [2000]. According to these authors, vanadium alloys provide favorable safety and environmental features such as low long-term activation, low decay heat and contact dose, and a potential for recycle. Vanadium alloys discussed by these investigators cover a broad range of compositions, V-(0-15)%Cr-(1-20)%Ti-(0-1)%Si, with particular emphasis given to a reference alloy, V-4Cr-4Ti. The three key alloying elements, vanadium, chromium and titanium, are mutually soluble in each other at elevated temperatures, and they all exhibit favorable low-activation characteristics.

When compared to austenitic stainless steels, ferritic steels, and silicon carbide, these materials have very favorable nuclear-related properties, as shown in Table 2. Vanadium alloys with a few percent titanium are resistant to irradiation-induced swelling and embrittlement at projected operating temperatures, and are said to be compatible with liquid-metal blanket/coolants. Helium and hydrogen transmutation rates in vanadium alloys are substantially less than those for other candidate materials exposed to high-energy neutrons characteristic of deuterium-tritium plasmas. Irradiation does harden the materials. For example, the yield stress of V-4Cr-Ti increases from the pre-irradiation level of 200-300 MPa to 600-700 MPa at a damage level of approximately 30 dpa, and temperatures of 430 to 600°C. The calculated contact doses for V-4Cr-4Ti, HT-9, SiC, after 5-year exposures to 5 MW/cm^2 for a fusion reactor first wall, are approximately 10^{-9}, 10^{-8}, 10^{-6}, and 10^{-5}, respectively.

The primary thermo-mechanical treatment of these alloys is a solution anneal at approximately 1000°C for one hour. Properties are relatively insensitive to annealing conditions for 950-1100°C for 0.5-2 hours. Thermal aging at temperatures ranging from 500 to 1000C, for exposure times up to 5000 hours, show no significant grain growth (grain size 20 ± 2 μm) [Smith et al. 2000]. In summary, candidate vanadium alloys exhibit good resistance to irradiation damage at temperatures of interest and offer a potential for long operating lifetime.

Other important physical properties of these candidate materials are summarized in Table 3 [Smith et al. 2000]. In particular, the coefficient of thermal expansion of V-Cr-Ti is lower than that of austentic and ferritic steels, which would help alleviate thermal stress and associated environmental cracking, and the thermal conductivity is significantly higher, which would help alleviate concerns regarding heat transfer.

Table 2 – Nuclear Related Properties of Candidate Structural Materials

Property	Type 316L Austenitic Steel	Type HT-9 Ferritic Steel	V-5Cr-5Ti Vanadium Alloy	Silicon Carbide
Melting Temperature (°C)	1400	1420	1880	2600[a]
Radiation Damage Rate [b] (dpa)	11	11	11	12
Helium Transmutation Rate [b] (appm)	174	130	57	1500
Hydrogen Transmutation Rate [b] (appm)	602	505	240	560
Nuclear Heating Rate [b] (W/cm^3)	11	11	7	11

Notes: [a] decomposition temperature; [b] fro 14 MeV neutron flux of 1 MW/m^2 for 1 year; and [c] for 14 MeV neutron flux of 1 MW/m^2.

Table 3 – Important Physical Properties of Candidate Structural Materials

Property	Type 316L Stainless Steel	Type HT-9 Ferritic Steel	V-Cr-Ti Alloy
Melting Temperature (°C)	1400	1420	1890
Density (g/cm^3)	8.0	7.8	6.1
Poisson's Ratio	0.27	0.27	0.36
Modulus of Elasticity (GPa at 400°C)	168	180	120
Linear Thermal Expansion (10^{-6}/K)			
400°C	17.6	11.8	10.2
500°C	18.0	12.3	10.3
600°C	18.3	12.6	10.5
Thermal Conductivity (W/m-K			
400°C	19.5	26.8	33.6
500°C	21.0	27.3	34.5
600°C	22.5	27.7	35.3
Electrical Resistivity (μm)			
400°C	1.01	0.91 [a]	0.67
500°C	1.06	0.99 [a]	0.74
600°C	1.12	1.05 [a]	
Specific Heat (J/kg-K)			
400°C	560	600	535
500°C	575	680	560
600°C	580	800	575

Notes: [a] data for Type 410 stainless steel.

Iron-Based and Nickel-Based Steels

Alloyed steels and high-alloyed steels are basic materials for structures [Ursu 1985, Section 12.5.2, p. 441]. The maximal temperature at which high-alloyed steels may still be used is ~1200°C. The relative shortcoming of their being affected by radioactivity implies storage problems for relatively long periods of time (~ 50 years). Austenitic steels with refractory metals, especially Cr, exhibit superior tensile properties at high temperatures. These steels are also corrosion resistant. When at extremely high temperatures, event the high-alloyed steels lose their strength and manifest a low formability. This is why at temperatures corresponding to the upper limit, they can only be used as protection, refractory materials.

In the temperature range of 400-550°C, pearlitic-ferritic steels are frequently used. To extend the range of operating temperatures to 450-550°C, it is necessary to increase the chromium (Cr) content to 3-3.5 weight percent (3-3.5%). Carbide-forming elements such as molybdenum, tungsten, and vanadium (Mo, W, and V) are also beneficial for extending the range of operating temperature. These steels are said to behave acceptably with hydrogen within this range of temperatures [Ursu 1985].

Ferritic stainless steels are essentially chromium-containing alloys with body -centered cubic (bcc) crystal structures [ASM Engineered Materials Handbook]. Chromium content is usually in the range of 10.5-30 weight percent (10.5-30%). Some grades contain molybdenum, silicon, aluminum, titanium, or niobium (Mo, Si, Al, Ti, or Nb) to confer particular characteristics. Ferritic alloys have good ductility and formability, but high-temperature strengths are relatively poor compared to those of austenitic grades. Toughness may be somewhat limited at low temperatures in heavy sections.

Unlike martensitic steels, ferritic stainless steels cannot be strengthened by heat treatment. Also, ferritic stainless steels are not often strengthened by cold work, because the strain-hardening rates of ferrite are relatively low and cold work significantly lowers ductility.

Typical annealed yield and tensile strengths for ferritic stai nless steels are 240 to 380 MPa (35 to 55 ksi) and 415 to 585 MPa (60 to 85 ksi), respectively. Ductilities end to range between 20 and 35 percent. Higher strengths, up to 515 MPa (75 ksi) for yield strength and 655 MPa (95 ksi) for tensile strength, are obtained in the more highly alloyed grades.

Whereas martensitic stainless steels offer only moderate corrosion resistance, that of ferritic stainless steels can range from moderate (for lower alloyed grades) to outstanidng (for more highly alloyed grades). Typical applications for ferritic stainless steels include equipment for handling oxidizing acids and organic acids, food processing equipment, and heat exchangers and piping used in seawater.

Note that this author does not specifically reference oxide-dispersion hardened (ODS) ferritic-martensitic (FM) steels, which may have slightly higher operating temperatures, due to the presence of the oxide particles, which prevent creep. Unfortunately, the corrosion resistance of ODS FM Steel appears to be no better than other ferrite steels. The dispersed oxide phase can be produced in various ways. For example, reverse micelle synthesis has been used as a means of making relatively large volumes of Y_2O_3 nano-particles for dispersion into iron-based amorphous alloys for similar purposes.

At higher temperatures, in the 500-600°C range, additional chromium is required. Chromium additions of 5-15 weight percent (5-15%) increase the re-crystallization temperature and prevent plastic deformation. For example, enhanced steels with 12 weight percent chromium (12% Cr) have been shown to behave well at an applied stress of 200 MPa and a temperature of 500°C for 10.000 hours At the upper limit of this temperature range, molybdenum, tungsten, vanadium and niobium (Mo, W, V or Nb) are needed [Ursu 1985].

Austenitic steel with 18% Cr, 9% Ni and 1% Ti, with carbides, can withstand an applied stress of 200 MPa at 630°C for 10,000 hour. Nickel alloys can be used as structural materials at temperatures up to 700°C, nickel-cobalt alloys can be used up to 800°C, and chromium alloys can be used up to 1100°C [Ursu 1985].

The maximum recommended operating temperature for high-alloyed steels is 1200°C. High chromium additions enhance not only the corrosion resistance of these materials, but also improve the high-temperature tensile properties. The properties of these materials are generally compromised by radiation damage. The following general guidance is provided for high-temperature applications of steels:

- Ferritic Steels (3-3.5% Cr): T < 400-550°C
- Other Steels (5-15% Cr): T < 500-600°C
- Iron-Based Austenitic Steels (9-12% Ni): T < 600-650°C
- Nickel-Based Alloys (Hastelloys A, N, X; Inconels; Others): T < 650-800°C

The following table summarizes published guidance regarding the levels of various alloying elements necessary to enhance oxidation resistance at various temperature levels. The maximum temperature is the temperature where substantial oxidation begins to occur.

Table 4. Guidance on Acceptable Compositions for Oxidation-Resistant Refractory Steels

Max. Temp. (°C)	Carbon (%)	Silicon (%)	Chromium (%)	Nickel (%)
850	0.35-0.45	2-3	8-10	
900	< 0.12	< 0.8	16-18	
950	0.25-0.34	2-3	12-14	6-7.5
1000-1050	< 0.2	2-3	19-22	12-15
1100-1150	< 0.15	< 1	27-30	

Refractory steels are used in the temperature range 900-1200°C, but cannot serve reinforcement purposes. Their strength depends upon temperature and increases with the rise in Cr concentration [Ursu 1985].

Corrosion of Structural Alloys by Blanket/Coolant/Fuel

In addition to having good high-temperature performance, such materials must also be chemically compatible with the blanket-cooling materials. The corrosion and chemical compatibility of candidate metals and alloys is summarized in Table 5 [Ursu 1985, Section 12.4.4, Table 12.17, p. 436].

Table 5 – Materials Compatibility with Coolants

	Liquid Li	Liquid Li	Li_2BeF_4
Alloy	Max. Temp. (°C)	Dissolved O_2 Effect	Corrosion Observed
Austenitic Steel	< 500		No
V Alloys	< 900	No	No
Mo Alloys	< 1100	No	No
Nb Alloys	< 1300	Yes	
Graphite	Incompatible		No

As discussed by Nishimura et al. [2001], FLIBE is considered as a candidate material for tritium breeding in a fusion liquid due to its chemical stability and low electrical conductivity. It has been selected for the conceptual design of the Force Free helical Reactor (FFHR). In this particular design, ferritic steel (Fe-9Cr-2W) and vanadium alloy (V-4Cr-4Ti) are the candidate materials for the blanket structure. In such applications, the tritium release behavior from FLIBE, and the corrosion of the structural materials by FLIBE are key to success.

As discussed by Cheng et al. [2003], corrosion problems start with the dissolution of the structural material in the coolant. The generalized oxidative corrosion reaction of reduced metal (M) with the molten fluoride salt (XF) is given as follows:

$$M + XF \rightarrow MF + X$$

In this reaction, X represents lithium, sodium, beryllium, or transmutation products, such as tritium. The transmutation of lithium produces hydrogen isotopes which react with free fluoride to form acid (HF, for example), making the blanket and coolant much more corrosive than it would otherwise be. The relative stability of various metals and alloys in fluoride salts can be understood in terms of the free energies of formation of various reaction products, as shown in Table 6. From this table of free energies, the following conclusions have been drawn by Cheng et al. [2003], and are repeated here. First, NaF, LiF and BeF2 are very stable salts. The metallic elements listed in the bable will not be able to react with them to form metallic salts. Second, hydrofluoric acid formed from transmutation products (TF/HF) will react the elements listed below HF in the table (free energy of formation more negative than TF/HF), but will not reat with the elements listed above HF (free energy of formation more positive than TF/HF). Therefore, vanadium, nickel, tungsten and molybdenum would be expected to be compatible with hydrofluoric acid (TF/HF). Finally, in the case of iron-based ferritic steel, with chromium, tungsten and titanium, free fluorine and hydrofluoric acid must be removed to prevent excessive corrosion of the structural material.

Table 6 – Free Energies of Formation for Various Fluorides

Fluoride Salts – Corrosion Products	Free Energy of Formation (kcal/g-mol F) at 1000K
MoF_6	-50.2
WF_6	-56.8
NiF_2	-55.3
VF_5	-58.0
VF_4	-66.0
HF	-66.2
FeF_2	-66.5
NbF_3	-72.5
CrF_2	-75.2
TaF_2	-82.2
TiF_4	-85.4
BeF_2	-106.9
LiF	-125.2
NaF	-129.0

Corrosion of Refractory Vanadium Alloys in Irradiated FLIBE

Thermochemical simulation, using the MALT2 data base and the GEM code, has also contributed to the understanding of vanadium alloy corrosion in FLIBE [Nishimura et al. 2001]. Chemical species predicted to form in the gas phase include: H_2, HF, H_2O, TiF_3, BeH_2, BeF_2, $LiBeF_3$. Here too the presence of metallic beryllium is predicted to suppress the formation of HF (and TF). Chemical species predicted to form in the condensed liquid phase due to the corrosion of ferritic stainless steel include: V, Cr, Ti, TiO, TiF_3, VF_3, BeO, Li_2BeF_4, and $LiBeF_3$. Titanium is preferentially attacked, and titanium and vanadium are volatilized as TiF3 and VF3, respectively. The formation of TiO scale could inhibit such corrosive attack. While increases in hydrogen partial pressure may reduce the rate of attack of iron in ferritic steels, there is little difference in the predicted outcomes for vanadium alloys in hydrogen and inert gas (argon) atmospheres. As in the case of ferritic steel corrosion in FLIBE, the presence of metallic beryllium has a positive effect on the formation of corrosive HF (and TF), it promotes formation of problematic gaseous BeH_2.

In experimental studies with vanadium, pits with diameters of approximately 200 microns were observed. After 10-day immersions, the alloy became brittle. X-ray diffraction did not show the formation of VF_2, VOF, or VO, which could have formed protective scales, but were not observed to do so. FLIBE is a very stable molten salt, however, under irradiation it forms acidic HF and TF, and causes severe corrosion of structural materials, including ferritic steels (specifically, Fe-9Cr-2W) and vanadium alloys (specifically, V-4Cr-4Ti). This does not necessarily rule out the design and fabrication of other high-performance ferritic and refractory alloys that could perform well in such environments. Alloys with elements forming less volatile fluoride species would be particularly interesting.

Electrochemical control, frequently using metallic beryllium, but possibly using metallic lithium or other reversible oxidation-reduction couples (mediators), may prove to be a useful means of controlling such corrosive attack. If beryllium is used, to formation of colloidal beryllium in the molten salt is problematic, in that it will thicken the solution. The formation of these particles is sufficiently great to cause such solutions to appear thick and grey.

Corrosion of Ferritic Steel in Irradiated FLIBE

Thermochemical simulation, using the MALT2 data base and the GEM code, has also contributed to the understanding of ferritic steel corrosion in FLIBE [Nishimura et al. 2001]. Chemical species predicted to form in the gas phase include: H_2, HF, $(HF)_2$, H_2O, FeF_3, BeH_2, BeF_2, $LiBeF_3$. The presence of metallic beryllium is predicted to suppress the formation of HF (and TF). Chemical species predicted to form in the condensed liquid phase due to the corrosion of ferritic stainless steel include: Fe, Cr, Fe_3W_2, Cr_2O_3, CrF_2, CrF_3, BeO, Li_2BeF_4, and $LiBeF_3$. Chromium is selectively attacked and depleted. Then, iron is fluorinated, and evaporates as the volatile FeF_3 species. There is some possibility that Cr_2O_3 could form a protective layer, suppressing the corrosion. Increasing hydrogen partial pressure could also suppress formation of volatile FeF_3. While the presence of metallic beryllium has a positive effect on the formation of corrosive HF (and TF), it promotes formation of problematic gaseous BeH_2.

Much of the corrosive nature of FLIBE is due to the formation of HF and TF through transmutation of the lithium-containing molten salt. The following observations of the corroded surface were made:

- X-ray Diffraction (XRD): α-Fe, Fe_2O_3 and spinel phases observed
- Rutherford Backscattering (RBS): oxygen penetration layer 200-nanometers thick
- Moessbauer Spectroscopy: formation of chromium depletion layer after 3-day immersion; the iron in oxide was trivalent, suggesting the formation of Fe_2O_3.

The investigators have constructed the following mechanism, based upon the experimental data. First, a layer of spinel-type oxide is formed on the surface. Then, a layer containing Cr_2O_3, $Fe(Fe,Cr)_2O_4$ and Fe_2O_3 grows, with a chromium depletion layer forming underneath.

Electrochemical Control of Oxidation State in Molten Salts

Electrochemical control, frequently using metallic beryllium, but possibly using metallic lithium or other reversible oxidation-reduction couples (mediators), may prove to be a useful means of controlling such corrosive attack. If beryllium is used, to formation of colloidal beryllium in the molten salt is problematic, in that it will thicken the solution. The formation of these particles is sufficiently great to cause such solutions to appear thick and grey.

It is believed that metallic beryllium and lithium reduce hydrofluoric acid (HF/TF) formed from lithium transmutation products, and therefore eliminates aggressive free fluoride anions from the melt, along with the corrosive attack of structural materials caused by these species. The reactions for beryllium and lithium are:

$$2TF + Be \rightarrow BeF_2 + T_2$$

$$2TF + 2Li \rightarrow 2LiF + T_2$$

Since more LiF than BeF_2 is consumed within the fusion reactor, the use of metallic lithium is the preferred method of reducing hydrofluoric acid and replenishing the lithium in the molten-salt blanket and coolant.

Other reduction-oxidation (redox) couples have also been considered for controlling free fluoride and corrosion in the blanket/coolant region, and include Ce(IV)/Ce(III), Eu(III)/Eu(II), and HF/F_2. However, these couples do not have a low enough fluoride potential to suppress TF formation to a level where corrosion is not a concern [Nishimura et al. 2001].

Cerium and other such oxidation-reduction couples were investigated by LLNL's Special Isotope Separation (SIS) Program in the early 1990's as a means of converting PuO_2 to PuO_4^{2+} (CEPOD or Silver Bullet Process) and as a means of destroying the organic fraction of mixed wastes (MEO Process) [Farmer et al. 1990-92].

The possibility of using metallic beryllium and lithium to control oxidation-reduction reactions in the molten salt is similar to the use of sacrificial anodes to control corrosion in aqueous environments. Such a parallel has also inspired the author to investigate the use of high-temperature cathodic protection systems to control both corrosion, as well as actinide volatilization, in the molten salt blanket and coolant in the hybrid fusion-fission reactor system. Such imposed currents could suppress corrosion current, and convert any potentially volatile hexavalent uranium species to the less volatile tetravalent form.

In essence, the beneficial effects observed by placing metallic beryllium in contact with neutron-irradiated FLIBE, with lithium transmutation products such as HF and TF can be understood, at least conceptually, by considering the electromotive series. As an example, consider the electrochemical reactions for beryllium, lithium, fluorine, iron, and hydrogen:

$Li^+ + e^- \leftrightarrow Li$	-3.045 V vs. SHE
$Be^{+2} + 2e^- \leftrightarrow Be$	-1.7 V vs. SHE
$Fe^{+2} + 2e^- \leftrightarrow Fe$	-0.409 vs. SHE
$2H^+ + 2e^- \leftrightarrow H_2$	+0.0 V vs. SHE
$F_2 + 2e^- \leftrightarrow 2F^-$	+2.85 V vs. SHE
$F_2 + 2H^+ + 2F^- \leftrightarrow 2HF$	+3.03 vs. SHE

Any electrochemical potential more negative (cathodic) than the stated Nernst potential will push the reactions to the right (reduction, acceptance of electron). Any electrochemical potential more positive (anodic) than the stated Nernst potential will push the reactions to the left (oxidation, liberation of electron by reduced metal or gas).

When two metals are galvanically coupled, a intermediate "mixed potential" is established. The exact position of this mixed potential, which is located between the redox potentials of the coupled metals, is determined by their relative electrode kinetics. The anodic and cathodic reactions are usually assumed to obey Tafel kinetics, and electro-neutrality must be preserved in the reactions. The intersection of the anodic and cathodic Tafel lines identifies the formal mixed potential. This will be the rest potential of both galvanically coupled metals. At this potential, one metal will undergo anodic dissolution, while the other will be cathodically protected, with the possible recombination of hydrogen ions on the surface. As an example, consider the zincs on your boats brass propeller, the less noble metal (zinc) will undergo anodic dissolution to protect the more noble metal from corrosion (brass or steel).

Hydrogen recombination on a metallic surface causes cathodic hydrogen charging, and sets the stage for hydrogen embrittlement and hydrogen induced cracking. In many metals, such as titanium, infused hydrogen diffuses up stress gradients to crack tips, forming brittle hydride phases. These brittle hydride phases periodically rupture under the stress at the crack tip, and enable crack propagation through the classical film rupture mechanism.

The same happens in FLIBE with the use of either beryllium or lithium. Note that both lithium and beryllium are less noble than iron and hydrogen. By galvanically coupling either metallic lithium or beryllium to iron, immersed in a blanket of FLIBE, a mixed potential will be established for the couple between the two redox potentials. This mixed potential will be more positive than the Nernst potential for the lithium/beryllium, and more negative thant the Nernst potential for the iron/hydrogen. Thus, the lithiium/beryllium will undergo preferential dissolution, while the hydrogen ions (from hydrofluoric acid species) will be converted to free fluoride anion and hydrogen gas, and the iron will be cathodically protected. Of course, this is a very simple minded explanation, and the above standard potentials (which are directly related to the Gibbs Free Energies for the reactions) are for aqueous solutions (solutions with hydrogen ions). However, they do provide sufficient insigt for a generalized understanding.

Now the interesting innovative part ... the use of sacrificial anodes on propellars or hybrid reactors is a form of passive electrochemical protection. The same can be accomplished with adder potentiostats (operational amplifiers with formal reference electrodes). Instead of relying on a sacrificial anode to maintain the surface to be protected at the appropriate potential, the potentiostat can be used to apply the potential through application of a carefully controlled current. Thus, the REDOX state of the ferritic steel, and transmuted lithium (H+ and T+) can be intentionally converted to the gaseous forms.

In addition to using the "electrochemical controller" to mitigate the corrosive effects of HF and TF, and the attack of structural materials, such REDOX control can also be used to manipulate the oxidation state of soluble uranium species (UF3, UF4 and UF6). Of course, we want to avoid the formation of the hexavalent uranium. In principle, you can use such electrochemical control to walk to various postions in the phase diagram.

A footnote - in such a cell, the fluoride would be removed by either; (1) electrolytic gas evolution; (2) continuously with a high-temperature ion exchanger, which are usually mineral phases in a column; or (3) electrochemically-controlled pairing with lithium ions ... bearing some similarity to the lithium sacrificial anode, except much more easily controlled, and safer. Note that metallic lithium has caused many explosions ... thus the introduction of graphite intercalation cathodes.

Note that we used large scale redox control for the electrochemically assisted dissolution of refractory plutonium oxide in the late 1980's and early 1990's for the SIS Program. The process was called CEPOD. This process was later converted to MEO for the electrochemical oxidation of the organic fraction of radioactive mixed wastes. In these processes, electrochemical cells (thousands of amps) were used to manipulate the redox potential of reversible couples involving silver, cerium, iron, and other species.

Such electrochemical control will require a detailed understanding to the electrochemical behavior of the electrolyte, dissolved fuel, and materials. This approach is discussed in the following section.

In Situ Studies of Corrosion Mechanism and Rates in FLIBE

As previously discussed, molten salts used as blanket/coolants in fusion-fission hybrid reactors become extremely corrosive through the transmutation of lithium in the blanket/coolant, which results in the formation of hydrofluoric acid species (HF and TF). The corrosion mechanisms of steels and refractory alloys in these electrolytes are not yet completely understood, however, reasonable assumptions can be made based upon published experimental data. The anodic process will probably involve the oxidative dissolution of metallic elements in the structural material, thereby forming dissolved metal cations. In the absence of oxygen, electrons generated by the anodic oxidation of the structural material must be consumed by some other electrochemical reduction process. Based upon published information, it is assumed that this cathodic reaction involves reduction of H^+ and T^+ cations and the formation of gaseous H_2 and HT. This reduction will liberate fluoride anions (F^-) which will then form ion pairs with dissolved metal cations produced by the anodic dissolution of metallic elements from the structural materials. Some of these metal fluoride salts will be in thermochemical equilibrium with volatile metal fluoride species.

First, the open-circuit potential (OCP), relative to a suitable high-temperature reference electrode, should be monitored as a function of immersion time. Note that the OCP corresponds the corrosion potential (E_{corr}), The linear polarization method should then be used as a means of monitoring the corrosion rates of various structural steels and refractory alloys immersed in FL:IBE and FLINABE. This approach will require that the relevant anodic and cathodic reactions must be established.

The pitting of steels and refractory alloys has been reported in FLIBE molten salts. Pitting of alloys is frequently associated with the localized destabilization of passive films with halide anions, such as fluoride, the reaction of such halide anions with relatively soluble inclusions in the alloy surface, or the localized reaction of such aggressive anions with specific active sites on the surface of an immune metal. In all cases, a threshold electrochemical potential exists, above which localized attack can occur.

Cyclic polarization is a convenient way to determine the threshold potential for steels and refractory alloys in high-temperature molten salts such as FLIBE. The resistance to such localized corrosion should be quantified through measurement of the open-circuit corrosion potential (E_{corr}), the threshold potential for localized attack ($E_{threshold}$), and the repassivation potential (E_{rp}), provided that the localized attack involves destabilization of a passive film, and provided that repassivation occurs during the cathodic branch of the polarization curve. Spontaneous breakdown of the passive film and localized corrosion require that the open-circuit corrosion potential exceed the critical potential:

$$E_{corr} \geq E_{threshold}$$

The greater the difference between the open-circuit corrosion potential and the critical potential (ΔE), the more resistant a material is to modes of localized corrosion such a pitting and crevice corrosion. In integrated corrosion models, general corrosion is invoked when E_{corr} is less than $E_{threshold}$ ($E_{corr} < E_{threshold}$), and localized corrosion is invoked when E_{corr} exceeds $E_{threshold}$. Measured values of the repassivation potential (E_{rp}) are sometimes used as conservative estimates of the critical potential ($E_{threshold}$).

To the extent possible, cyclic polarization (CP) measurements should be conducted in accordance with ASTM (American Society for Testing and Materials) G-5 and other similar standards, with slight modification [27]. The ASTM G-5 standard calls for a 1N H_2SO_4 electrolyte, whereas measurements for the fusion-fission hybrid reactor will be made in FLIBE or FLINABE, with the possible addition of UF_4 as fissionalble fuel. In the absence of high fluxes of fast neutrons, the effects of transmutation will be simulated by adding hydrogen fluoride to and inert purge gas that will be bubbled through the cell.

The procedure used for linear polarization testing consisted of the following steps: (1) holding the sample for ten seconds at the OCP; (2) beginning at a potential 20 mV below the OCP, increasing the potential linearly at a constant rate of 0.1667 mV per second to a potential 20 mV above the OCP; (3) recording the current being passed from the counter electrode to the working electrode as a function of potential relative to an appropriate high-temperature reference electrode; and (4) determining the parameters in the cathodic Tafel line by performing linear regression on the voltage-current data, from 10 mV below the OCP, to 10 mV above the OCP. The slope of this line was the polarization resistance, *Rp* (ohms), and was defined in the published literature [Treseder 1991].

$$R_P = \left(\frac{\partial E}{\partial I} \right)_{E_{corr}}$$

A parameter (*B*) was defined in terms of the anodic and cathodic slopes of the Tafel lines:

$$B = \frac{\beta_a \beta_c}{2.303(\beta_a + \beta_c)}$$

The corrosion current density, i_{corr} (A cm^{-2}), was defined in terms of the Tafel parameter (B), the polarization resistance (Rp), and the actual electrode area (A):

$$i_{corr} = \frac{B}{R_p \times A}$$

The corrosion (or penetration) rates of the amorphous alloy and reference materials were calculated from the corrosion current densities with the following formula:

$$\frac{dp}{dt} = \frac{i_{corr}}{\rho_{alloy} n_{alloy} F}$$

where p was the penetration depth, t was time, i_{corr} was the corrosion current density, ρ_{alloy} was the density of the alloy (g cm^{-3}), n_{alloy} was the number of gram equivalents per gram of alloy, and F was Faraday's constant. The value of n_{alloy} was calculated with the following formula:

$$n_{alloy} = \sum_j \left(\frac{f_j n_j}{a_j} \right)$$

where f_j was the mass fraction of the j^{th} alloying element in the material, n_j was the number of electrons involved in the anodic dissolution process, which was assumed to be congruent, and a_j was the atomic weight of the j^{th} alloying element. Congruent dissolution was assumed, which meant that the dissolution rate of a given alloy element was proportional to its concentration in the bulk alloy. These equations were used to calculate factors for the conversion of corrosion current density to the penetration rate (corrosion rate).

A temperature controlled electrochemical cell will be required for cyclic and linear polarization tests, as well as for electrochemical impedance spectroscopy. This cell will be constructed to operate at temperatures well above the melting point of Li_2BeF_4. This cell should have three electrodes, a working electrode (test specimen), a reference electrode, and a counter electrode. An appropriate high-temperature reference electrode should be used. This reference electrode should be a reversible half cell, with an electrolyte that shares common ions (Li^+, Be^{+2} and F^-) with FLIBE, communicates with the test solution via a Luggin probe or ion-conductive membrane placed in close proximity to the working electrode, constructed in a way to minimize Ohmic losses, and connected to the potentiostat through a very high impedance, to avoid perturbation of the standard half-cell reaction. The three-electrode electrochemical cell should be equipped with a temperature-controlled junction to maintain the standard reference electrode at a known temperature, which will thereby maintain integrity of the potential measurement. The gas phase should be continuously monitored with a quadrapole mass spectrometer (QMS) to determine the concentration of volatile corrosion products accumulating in the gas phase.

Radiation Effects in Structural Materials

Radiation Swelling of Ferritic Steels

An annealed and aged ferritic steel which was dispersion hardened with fine niobium carbide (NbC) precipitates, and contained relatively coarse particles of Laves phase, was bombarded with a 4-MeV beam of iron ions [Farrell et al. xxx]. The damage level was 100 displacements per atom (100 dpa) at 400-600°C. Much of the damaged structure consisted of dislocation tangels that coarsened with increasing temperature. Cavity formation began at 450°C, appeared to peak at approximately 535°C, and was absent at 600°C. The maximum swelling observed during these tests was only 0.2 percent (0.2 %). The Laves particles exhibited recoil dissolution and restructuring.

Bombardments with iron, helium and deuterium (Fe, He, and D) beams or iron and helium (Fe and He) beams, at ratios of 10 and 45 atomic parts per million (appm) He/dpa, introduced high concentrations of small bubbles and comparatively few large bias-driven cavities. The latter were initiated at bubble clusters on niobium carbide (NbC) particles. The maximum extent of swelling was 0.75% and occurred at 550°C. Recoil dissolution of the Laves phase was retarded by the gases. Large critical cavity sized and an unbalanced dislocation and cavity sink strengths contributed to low swelling of this alloy.

Nickel-Based Alloys

The irradiation induced swelling of the Inconel 600 and 316 stainless steel reflector components and the consequences of this swelling on the performance of the reflector assemblies is described in the literature [Makenas et al. 1986]. Transmission electron microscopy samples of Inconel 600 wee prepared from two of the swelling samples used to generate the data in Figure 12. Limited void swelling was found in the low fluence specimen, while extensive voidage was found in the higher fluence, middle-of-core specimen. A comparison of the swelling measured by immersion density versus that obtained by microscopy measurement is given in Table 7. The voids exhibit the truncated octahedral shapes normally found in face-centered cubic alloys. Neither transmisison electron microscopy nor the subsequent topical metallographic examination for second phases were helpful in determining the irradiation te4mperature of these specimens since Inconel 600 is not prone to temperature dependent phase changes, which might indicate a specific temperature.

Table 7 – Radiation Swelling of Inconel 600 [Makenas et al. 1986, Table 1, Figure 11]

Material	Specimen Fluence (n cm^{-2})	Vol. Change by Immersion (%)	Vol. Change by TEM (%)	Data Source
Inconel 600	1×10^{22} n cm^{-2} at E > 0.1 MeV	3.6 %	5.0 %	Table 1
Inconel 600	1×10^{22} n cm^{-2} at E > 0.1 MeV	0.32%	< 0.1%	Table 1
Inconel 600	1×10^{22} n cm^{-2} at E > 0.1 MeV	< 0.5%		Fig. 11
Inconel 600	4×10^{22} n cm^{-2} at E > 0.1 MeV	1%		Fig. 11
Inconel 600	7×10^{22} n cm^{-2} at E > 0.1 MeV	2%		Fig. 11
Inconel 600	9×10^{22} n cm^{-2} at E > 0.1 MeV	5%		Fig. 11

Radiation Swelling of Beryllium

The general experience with beryllium (Be) is that it will swell and crack after receiving relatively low radiation doses, and that these problems will preclude its use for any structural function at doses as high as 200 dpa [Moyer 2007]. Beryllium swells by T and He produced during transmutation. At approximately 600°C, beryllium begins to release tritium (T), and continues the release up to 900°C. If beryllium is used only non-structural components, such as pebbles or high-porosity metallic foams, with no requirements for strength and stability, problems associated with radiation-induced swelling will be inconsequential [Caro 2007].

Other High-Temperature Materials as Building Blocks

In the future, new high-performance first-wall composite materials could exploit the high melting points, and low vapor pressures of a broad range of known compounds. These compounds fall into several broad classes, including carbides, nitrides, oxides, intermetallics and silicides.

- Carbides
    - 3500-4000°C: (Ta,Cr,Zr)C, HfC, Tac, ZrC, NbC
    - 3000-3500°C: Ta_2C, TiC
    - 2500-3000°C: SiC, VC, W_2C, MoC, ThC_2, WC
    - 2000-2500°C: B_4C, Al_4C_3
    - 1500-2000°C: Te_3C
- Nitrides
    - 3000-3500°C: HfN, TaN, BaN
    - 2500-3000°C: ZrN, TiN, UN, ThN
    - 2000-2500°C: AlN, Be3N, NbN, VN
- Borides
    - 3000-3500°C: HfB, TaB_2, ZrB_2, NbB_2
    - 2500-3000°C: TiB_2, Ta_3B_4
    - 2000-2500°C: VB_2, TaB, WB, W_2B_5, TiB, MoB, CrB_2, MoB_2, CrB, Ta_3B_2, TiB, Mo_2B
- Intermetallics
    - 3000-3500°C: Re_5W_2
    - 2500-3000°C: MoW
    - 2000-2500°C: CrAl, Mo_3Al, UBe_2, Zr_5Sn_3
    - 1500-2000°C: Cr_3Ta, NiAl
- Silicides
    - 2500-3000°C: Ta_3Si
    - 2000-2500°C: $TaSi_2$, W_5Si_3, Zr_2Si, WSi_2, ZrSi, V_3Si, Mo_3Si, Mo_4Si, $MoSi_2$

Advanced Shielding Materials

The high boron content of $Fe_{49.7}Cr_{17.7}Mn_{1.9}Mo_{7.4}W_{1.6}B_{15.2}C_{3.8}Si_{2.4}$ (SAM2X5) makes it an effective neutron absorber, and suitable for criticality control applications. Average measured values of the neutron absorption cross section in transmission (Σ_t) for Type 316L stainless steel, Alloy C-22, borated stainless steel, a Ni-Cr-Mo-Gd alloy, and SAM2X5 have been determined to be approximately 1.1, 1.3, 2.3, 3.8 and 7.1, respectively [22]. This material and its parent alloy have been shown to maintain corrosion resistance up to the glass transition temperature, and to remain in the amorphous state after receiving relatively high neutron dose.

Materials used in criticality control applications must be relatively stable during irradiation with thermal neutrons. Melt-spun ribbon samples of various iron-based amorphous metals were subjected to high neutron dose in the 1.5 MW TRIGA reactor at McClellan Nuclear Radiation Center (MNRC) [22]. The neutron flux was 1.6×10^{10} n cm^{-2} sec^{-1}. Samples were irradiated for three different times: duration of 1st irradiation was 44 minutes; duration of 2nd irradiation was 132 minutes; and duration of 3rd irradiation was 263 minutes. The corresponding neutron doses were: 4.3×10^{13} n cm^{-2}, 1.3×10^{14} n cm^{-2} sec^{-1} and 2.6×10^{14} n cm^{-2}, respectively. These doses are equivalent to approximately 670, 2000 and 4000 years inside the waste packages designed for emplacement at Yucca Mountain. An exposure corresponding to a 4000-year service life does not cause any detectable, deleterious phase transformations.

Cost of Advanced Materials

A cost model was developed and used to predict the cost to produce nickel-based alloys, including Type 316 stainless steel, as well as nickel-based Alloys C-276 and C-22. This cost model used raw materials data compiled by the United States Geological Survey (USGS), and represented graphically in the following figure.

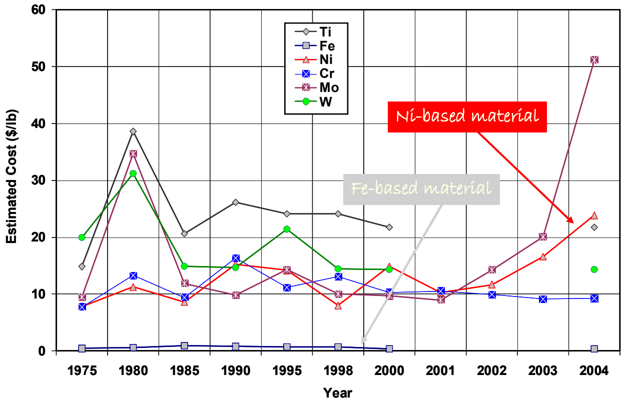

Figure 1. Cost of raw materials required for the production of ferritic and austenitic steels, nickel-based alloys, and various refractory alloys. These costs were provided by the United States Geological Survey (USGS).

Discussion

Failure of mechanical pumping system would result in collapse of the vortex. The vortex concept works against gravity.

Maintaining vortex with liquid – thickening with corrosion products and the roughening of the first wall may make vortex formation difficult.

A cylindrical reaction vessel, with the centerline oriented in the same direction as the gravitational field, would enable the design of reaction vessels with falling liquid films protecting the vessel walls. Such a system could be gravity fed and designed to maintain laminar flow, thereby avoiding the formation of problematic aerosols with the turbulent flow field.

Volatilization of the molten salt, corrosion products, and uranium fuel will probably foul optical windows and transparent blast shields. As a minimum precaution, very long optical paths, differential pumping, electrostatic precipitators, and shutters will probably be required.

The transmutation of lithium in the molten salt will form extremely corrosive HF and TF, which will attack the most corrosion resistant steels and refractory alloys. Very clever alloy designs, and corrosion mitigation approaches, including high-temperature sacrificial anodes and cathodic protection systems will be required to mitigate corrosion.

Joining of alloy with welding techniques will probably be used to construct the hybrid reactor. Residual weld stress, as well as thermal stresses caused by differential heating, will drive environmental cracking processes. Radiation damage and the formation of Such environmental cracking processes will include (1) hydrogen induced cracking and (2) stress corrosion cracking.

If spherical fuel particles are used (TRISO, for example), large number of spherical fuel particles (10^8 to 10^9) with high rate of inspection (50Hz) and modest rejection rate may require huge refurbishing (reprocessing) plant

- Inspect 50 Particles Per Second
- Assume Rejection 2.5%
- Required Refurbishing Rate
    - ~ 12,000 particles/day
    - ~ 130 kilograms/day

References

T. Angeliu, J. Ward and J. Witter, Assessing the Effects of Radiation Damage on Ni-Base Alloys for the Prometheus Space Reactor System, LM-06K033, April 4th 2007 (Knolls Atomic Power Laboratory, KAPL, Lockheed Martin, P. O. Box 1072, Schenectady, New York 12301-1072, Telephone 518-395-6163, Email angeltm@kapl.gov.

ASM Engineered Materials Handbook, ASM International, pp. 116-117

E. T. Cheng, B. J. Merril, Dai-Kai Sze: Nuclear aspects of molten salt blankets, Fusion Engineering and Design, Fusion Engineering and Design 69 (2003) 205-213.

J. C. Farmer: Electrochemical treatment of mixed and hazardous wastes, Chapter in Environmental Oriented Electrochemistry, Studies in Environmental Science 59, Edited by C. A. C. Sequeira (Elsevier, New York, New York, 1994) pp. 565-600.

J. Farmer, S. Lu, D. McCright, G. Gdowski, F. Wang, T. Summers, P. Bedrossian, J. Horn, T. Lian, J. Estill, A. Lingenfelter, W. Halsey, General and Localized Corrosion of High-Level Waste Container in Yucca Mountain, Transportation, Storage, and Disposal of Radioactive Materials, ASME, PVP Vol. 408, 2000, pp. 53-70

J. Farmer, J. Haslam, S. Day, T. Lian, R. Rebak, N. Yang, L. Aprigliano, Corrosion Resistance of Iron-Based Amorphous Metal Coatings, PVP2006-ICPVT11-93835, ASME, New York, NY, 2006

J. Farmer, J. Haslam, S. Day, D. Branagan, C. Blue, J. Rivard, L. Aprigliano, N. Yang, J. Perepezko, M. Beardsley, Corrosion Characterization of Iron-Based High-Performance Amorphous-Metal Thermal-Spray Coatings, PVP2005-71664, ASME, New York, NY, 2005

J. Farmer, J. Haslam, S. Day, T. Lian, C. Saw, P. Hailey, J. Choi, R. Rebak, N. Yang, R. Bayles, L. Aprigliano, J. Payer, J. Perepezko, K. Hildal, E. Lavernia, L. Ajdelsztajn, D. Branagan and M. Beardsely, A High-Performance Corrosion-Resistant Iron-Based Amorphous Metal – The Effects of Composition, Structure and Environment on Corrosion Resistance, *Scientific Basis for Nuclear Waste Management XXX*, Symposium NN, MRS Symposium Series, Vol. 985, 2006

J. Farmer, J. Haslam, S. Day, T. Lian, C. Saw, P. Hailey, J. Choi, N. Yang, C. Blue, W. Peter, J. Payer and D. Branagan, Corrosion Resistances of Iron-Based Amorphous Metals with Yttrium and Tungsten Additions in Hot Calcium Chloride Brine and Natural Seawater, $Fe_{48}Mo_{14}Cr_{15}Y_2C_{15}B_6$ and W-containing Variants, *Critical Factors in Localized Corrosion 5, A Symposiun in Honor of Hugh Issacs, 210th ECS Meeting*, edited by N. Missert, ECS Transactions, Vol. 3, ECS, 2006

K. F. Farrell and E. H. Lee: Ion damage in a Fe-10Cr-6Mo-0.5Nb ferritic steel, *Radiation-Induced Changes in Microstructure, 13th International Symposium, Part I*, Garner, Packan, Kumar, Editors, ASTM STP 955 (American Society for Testing and Materials, ASTM, Philadelphia, Pennsylvania, 1986) pp. 498-519.

T. Lian, D. Day, P. Hailey, J. Choi and J. Farmer, Comparative Study on the Corrosion Resistance of Fe-Based Amorphous Metal, Borated Stainless Steel and Ni-Cr-Mo-Gd Alloy, *Scientific Basis for Nuclear Waste Management XXX*, Symposium NN, MRS Series, Vol. 985, 2006

A. Caro, Chemistry, Materials and Life Sciences Directorate, Lawrence Livermore National Laboratory, 7000 East Avenue, Livermore, California 94551, Telephone 925-422-1711, Email caro2@llnl.gov.

J. Choi, C. Lee, J. Farmer, D. Day, M. Wall, C. Saw, M. Boussoufi, B. Liu, H. Egbert, D. Branagan, and A. D'Amato, Application of Neutron-Absorbing Structural Amorphous Metal Coatings for Spent Nuclear Fuel Container to Enhance Criticality Safety Controls, *Scientific Basis for Nuclear Waste Management XXX*, Symposium NN, MRS Symposium Series, Vol. 985, 2006

J. Farmer, J. Haslam, S. Day, T. Lian, C. Saw, P. Hailey, J. Choi, R. Rebak, N. Yang, J. Payer, J. Perepezko, K. Hildal, E. Lavernia, L. Ajdelsztajn, D. Branagan, Corrosion Resistance of Thermally Sprayed High-Boron Iron-Based Amorphous-Metal Coatings: $Fe_{49.7}Cr_{17.7}Mn_{1.9}Mo_{7.4}W_{1.6}B_{15.2}C_{3.8}Si_{2.4}$, J. Materials Research, 2007 (Accepted for Publication).

J. C. Farmer, J-S. Choi, C-K. Saw, R. H. Rebak, S. D. Day, T. Lian, P. D. Hailey, J. H. Payer, D. J. Branagan, L. F. Aprigliano, Corrosion Resistance of Amorphous $Fe_{49.7}Cr_{17.7}Mn_{1.9}Mo_{7.4}W_{1.6}B_{15.2}C_{3.8}Si_{2.4}$ Coating, A New Criticality Control Material, UCRL-JRNL-229505, LLNL, Livermore, CA; J. Nuclear Technology, 2007 (Accepted for Publication).

W. R. Grimes, S. Cantor: Molten salt as blanket fluids in controlled fusion reactors, The Chemistry of Fusion Technology, Plenum Press, 1972.

P. N. Haubenreich, J. R. Engel: Experience with the molten-salt reactor experiment, Nuclear Applications and Technology 8 (1970) 118-121.

J. E. Indacochea, J. L. Smith, K. R. Litko, E. J. Karell: Corrosion performance of ferrous and refractory metals in molten salts under reducing conditions, Journal of Materials Research 14, 5 (1999) 1990-1995.

B. J. Makenas, R. G. Trenchard, S. L. Hecht, J. M. McCarthy and F. A. Garner: The effect of swelling in Inconel 600 on the performance of FFTF reflector assemblies, *Radiation-Induced Changes in Microstructure, 13th International Symposium, Part I*, Garner, Packan, Kumar, Editors, ASTM STP 955 (American Society for Testing and Materials, ASTM, Philadelphia, Pennsylvania, 1986) pp. 206-229.

H. Nishimura, A. Suzuki, T. Terai, M. Yamawaki, S. Tanaka, A. Sagra, O. Motojima: Chemical behavior of Li_2BeF_4 molten salt as a liquid tritium breeder, Fusion Engineering and Design 58-59 (2001) 667-672.

H. Okamoto: Desk Handbook of Phase Diagrams for Binary Diagrams (American Society of Metals, International, Materials Park, Ohio, 2000)

D. A. Petti, G. R. Smolik, M. F. Simpson, J. P. Sharpe, R. A. Andrerl, S. Fukada, Y. Hatano, M. Hara, Y. Oya, T. Terai, D-K. Sze, S. Tanaka: Jupiter-II molten salt FLIBE research, an update on trituium, mobilization and redox chemistry experiments: Fusion Engineering and Design 81 (2006) 1439-1449.

B. A. Pint, P. F. Tortorelli, A. Jankowski, J. Hayes, t. Muroga, A. Suzuki, O. I. Yeliseyeva, V. M. Chernov: Recent progress in the development of electrically insulating coatings for a liquid lithium blanket, journal of Nuclear Materials 329-333 (2004) 119-124.

B. A. Pint, J. L. Moser, P. f. Tortorelli: Liquid metal compatibility issues for test blanket modules, Fusion Engineering and Design 81 (2006) 901-908.

D. L. Smith, M. C. Billone, K. Natesan: Vanadium-base alloys for fusion first-wall/blanket applications, International Journal of Refractory Metals and Hard Materials 18 (2000) 213-224.

A. Suzuki, T. Muroga, B. A. Pint, T. Yoneoka, S. Tanaka: Corrosion behavior of AlN for self-cooled Li/V blanket application, Fusion Engineering and Design 69 (2003) 397-401.

I. N. Sviatoslavsky, M. E. Sawan, E. A. Mogahed, S. Majumdar, R. Mattas, S. Malang, P. J. Fogarty, M. Friend, C. P. C. Wong and S. Sharafat: Engineering and geometric aspects of the solid wall re-circulating fluid blanket based on advanced ferritic steel, Fusion Engineering and Design 72 (2004) 307-326.

R. Treseder, R. Baboian, and C. Munger: Polarization resistance method for determining corrosion rates, *Corrosion Engineer's Reference Book*, 2nd Ed. (National Association of Corrosion Engineers, NACE, Houston, Texas, 1991) pp. 65-66

Ioan Ursu: Materials in fusion reactors, Chapter 12, *Physics and Technology of Nuclear Materials* (Pergamon Press, New York, New York, 1985) pp. 406-457.

S. J. Zinkle and N. M. Ghoniem: Operating temperatue windows for fusion reactor structural materials, Fusion Engineering and Design, 51-51 (2000) 55-71.

Appendix A

Patent Search: Fusion Reactor + First Wall

Hit	U.S. Patent	Title
1	7,193,228	EUV light source optical elements
2	7,128,980	Composite component for fusion reactors
3	7,037,464	Dispersed oxide reinforced martensitic steel excellent in high temperature strength and method for production thereof
4	6,824,888	Bonded body comprising beryllium member and copper or copper alloy member, and method of manufacturing the same
5	6,565,988	Composite for high thermal stress
6	6,495,002	Method and apparatus for depositing ceramic films by vacuum arc deposition
7	6,489,027	High purity carbon fiber reinforced carbon composites and manufacturing apparatus for use thereof
8	6,411,666	Method and apparatus to produce and maintain a thick, flowing, liquid lithium first wall for toroidal magnetic confinement DT fusion reactors
9	6,350,702	Fabrication process of semiconductor substrate
10	6,294,478	Fabrication process for a semiconductor substrate
11	6,246,740	SIC-composite material sleeve and process for producing the same
12	5,987,088	Precipitation hardening type single crystal austenitic steel, and usage the same
13	5,901,336	Bonding beryllium to copper alloys using powder metallurgy compositional gradients
14	5,779,822	Precipitation hardening type single crystal austenitic steel
15	5,736,198	Self-recoverable covering material and method for fabricating the same
16	5,681,511	Hermetic ceramic composite structures
17	5,589,652	Ceramic-particle-dispersed metallic member, manufacturing method of same and use of same
18	5,586,152	Carbon fiber-reinforced carbon composite materials, processes for their production, and first walls of nuclear fusion reactors employing them
19	5,583,900	Structural member having superior resistance to neutron irradiation embrittlement, austenitic steel for use in same, and use thereof
20	5,581,039	Ceramic body and method and apparatus for detecting change thereof
21	5,580,658	Copper-carbon composite material with graded function and method for manufacturing the same
22	5,447,683	Braze for silicon carbide bodies
23	5,445,803	Method and a device for decomposing tritiated water and for recovering

		elementary tritium
24	5,410,574	Internal component of fusion reactor
25	5,390,217	Carbon fiber-reinforced carbon composite materials processes for their production, and first walls of nuclear fusion reactors employing them
26	5,316,597	A nuclear reactor comprising a reactor vessel and structural members made of an austenitic stainless steel having superior resistance to irradiation-induced segregation
27	5,292,384	Cr-W-V bainitic/ferritic steel with improved strength and toughness and method of making
28	5,285,484	Remote control apparatus for maintaining in-vessel components in a structure having an inner torus space
29	5,278,881	Fe-Cr-Mn Alloy
30	5,203,932	Fe-base austenitic steel having single crystalline austenitic phase, method for producing of same and usage of same
31	5,202,158	Apparatus for and method of producing high density fiber reinforced composite material
32	5,182,075	Nuclear fusion reactor
33	5,174,945	Controlled thermonuclear fusion power apparatus and method
34	5,173,248	Remote control apparatus for maintaining in-vessel components in a structure having an inner torus space
35	5,116,569	Austenitic steel excellent in resistance to neutron irradiation embrittlement and members made of the steel
36	5,049,350	Controlled thermonuclear fusion power apparatus and method
37	5,023,043	Actively cooled device
38	5,019,321	Modular fusion power apparatus using disposable core
39	5,015,432	Method and apparatus for generating and utilizing a compound plasma configuration
40	5,012,860	Actively cooled heat protective shield
41	4,989,773	Method of joining graphite and metallic material with a material comprising titanium, nickel and copper
42	4,981,761	Ceramic and metal bonded composite
43	H845	Advanced vanadium alloys for magnetic fusion applications
44	H807	Manganese-stabilized austenitic stainless steels for fusion applications
45	4,928,755	Microtube strip surface exchanger
46	4,885,128	Method for improving performance of irradiated structural materials
47	4,867,762	Method and a device for purifying a gas containing hydrogen isotopes
48	4,859,399	Modular fusion power apparatus using disposable core
49	4,858,817	Graphit-ceramic RF Faraday-thermal shield and plasma limiter
50	4,852,645	Thermal transfer layer

Appendix B

Literature Search: Fusion Reactor + First Wall Materials

Author: Abe, K.; Masuyama, T.; Satou, M.; Hamilton, M. L.

Year: 1993

Title: Neutron-Irradiation Damage and Void Lattice Formation in a Molybdenum Alloy Tzm

Journal: Materials Transactions Jim

Volume: 34

Issue: 11

Pages: 1137-1142

Date: Nov

Accession Number: ISI:A1993MP11100022

Abstract: Molybdenum alloys are candidate materials for high heat flux components of fusion reactors. In order to study the neutron irradiation damage at high fluence levels, disks of the molybdenum alloy TZM that had been stress relieved at 1199 K for 0.9 ks were irradiated in the FFTF/MOTA at 679, 793 and 873 K to a neutron fluence of 9.6 x 10(26) n/m(2) (E(n)>0.1 MeV). Defect microstructures were observed by transmission electron microscopy. Dislocation structures consisted of isolated loops, aggregated loops (rafts) and elongated dislocations. The size of the loops increased with the irradiation temperature. The levels of void swelling were 0.68 and 1.6% at 793 and 873 K, respectively. A void lattice was developed in the body-centered-cubic (b.c.c.) structure with a lattice spacing of 28 nm. The fine grain size (0.5-2 mu m) was retained following high-temperature irradiation, indicating that the stress relief heat treatment may extend the material's resistance to irradiation damage up to high fluence levels. The relationship between the microstructure and irradiation hardening was determined.

Author: Bilous, O. A.; Artyukh, L. V.; Velikanova, T. Y.; Bryskin, B. D.

Year: 1999

Title: New high-temperature heat-resistant alloys on the basis of the Cr-Ti-C system

Journal: International Journal of Refractory Metals & Hard Materials

Volume: 17

Issue: 4

Pages: 259-263

Accession Number: ISI:000082241800002

Abstract: The outlook is good for the structure and mechanical properties of eutectic alloy Cr-Ti-C in the temperature range from 200 to 1200 degrees C as high-temperature material has shown. The possibilities of increasing high-temperature strength of Cr-Ti-C alloy by alloying with iron, scandium, lanthanum, molybdenum, and rhenium are discussed. (C) 1999 Elsevier Science Ltd. All rights reserved.

Author: Cardarelli, F.; Taxil, P.; Savall, A.; Comninellis, C.; Manoli, G.; Leclerc, O.

Year: 1998

Title: Preparation of oxygen evolving electrodes with long service life under extreme conditions

Journal: Journal of Applied Electrochemistry

Volume: 28

Issue: 3

Pages: 245-250

Date: Mar

Accession Number: ISI:000072076300004

Abstract: Among the numerous base metals tested for DSA(R) type electrodes (e.g., titanium and its alloys, zirconium, niobium etc.), tantalum is a potentially excellent substrate owing to its good electrical conductivity and corrosion resistance, and the favourable dielectric properties of its oxide. Nevertheless, a DSA(R) type electrode fabricated on a tantalum substrate would be very expensive due to the high cost of the metal. To prepare an anode combining the excellent properties of tantalum at reasonable price, a new material has been developed in our laboratory. This consists of a common base metal (e.g., Cu) covered with a thin tantalum coating. This tantalum layer was obtained by molten salt electroplating in a LiF-NaF-K2TaF7 melt at 800 degrees C. Thus, an anode of the type Metal/Ta/Ta2O5-IrO2 with a surface load of 22 g m(-2) IrO2, submitted to the severe test conditions used in this work, exhibits a standardized lifetime tenfold greater than one made with ASTM grade 4 titanium base metal. Thus, this type of electrode might be advantageously employed as an oxygen evolution anode in acidic solutions.

Author: Cheng, E. T.; Merril, B. J.; Sze, D. K.

Year: 2003

Title: Nuclear aspects of molten salt blankets

Journal: Fusion Engineering and Design

Volume: 69

Issue: 1-4

Pages: 205-213

Date: Sep

Accession Number: ISI:000185638700037

Abstract: Nuclear aspects of candidate molten salts, namely a mixture of LiF and BeF2 (FLIBE) and a mixture of LiF, NaF, and BeF2 (FLINABE), were investigated for application as blanket coolants in tokamak fusion power plants. Tritium breeding, blanket energy multiplication, and neutron transmutation of these salts were assessed. Neutron activation of FLIBE and FLINABE was evaluated and site-boundary dose due to a worst-case loss of vacuum accident was estimated. Formation of F-2, TF and T-2 during power plant operation was analyzed and issues relevant to corrosion of structural materials due to the fluorine and fluoride species was assessed. Mechanism to control the corrosion of structural materials due to TF has been identified. Depletion of LiF, BeF2, and NaF in the salts was calculated and quantities of the make-up fluorides to be added into the salts were estimated. (C) 2003 Elsevier B.V. All rights reserved.

Author: Cuthbertson, J. W.; Langer, W. D.; Motley, R. W.

Year: 1992

Title: Reflection of Low-Energy Plasma Ions from Metal-Surfaces

Journal: Journal of Nuclear Materials

Volume: 196

Pages: 113-128

Date: Dec

Accession Number: ISI:A1992KG25000014

Abstract: Reflection of low energy (< 100 eV) ions from surfaces plays an important role in areas of plasma technology such as in the edge region of fusion devices. We have developed a beam source based on acceleration and reflection of ions from a magnetically confined coaxial rf plasma source. The beam provides a large enough ion flux (over 4 A) to allow the characteristics of the reflected neutrals to be measured despite the inefficiency of detection. The energy distributions are measured by means of an electrostatic cylindrical mirror analyzer coupled with a quadrupole mass spectrometer. Energy distributions have been measured for oxygen, nitrogen and inert gas ions incident with from 10 to 70 eV reflected from amorphous metal surfaces of several compositions. The characteristics of particle reflection are commonly predicted in plasma modelling by use of simulation codes based on data from much higher incident energies. Measurements on this beam source allow the assumptions and approximations used in such codes to be tested. The predictions of the widely used TRIM code are compared to measured reflected energy distributions at low incident energies; significant differences are observed, particularly for lower target/projectile atomic mass ratios. The adequacy of the sequential binary collision approximation (used by TRIM) for modelling a collision process which at low energies is actually a simultaneous interaction between several atoms is tested by comparison with n-body trajectory calculations.

Author: Cuthbertson, J. W.; Motley, R. W.; Langer, W. D.

Year: 1992

Title: High-Flux Source of Low-Energy Neutral Beams Using Reflection of Ions from Metals

Journal: Review of Scientific Instruments

Volume: 63

Issue: 11

Pages: 5279-5288

Date: Nov

Accession Number: ISI:A1992JW82200009

Abstract: Reflection of low-energy (< 100 ev) ions from surfaces can be applied as a method of producing high-flux beams of low-energy neutral particles, and is an important effect in several areas of plasma technology, such as in the edge region of fusion devices. We have developed a beam source based on acceleration and reflection of ions from a magnetically confined coaxial rf plasma Source. The beam provides a large enough flux (over 4 A ion current, or 5 X 10(16) atoms/cm2 s at 10-cm range) to allow the energy distribution of the reflected neutrals to be measured despite the inefficiency of detection, by means of an electrostatic cylindrical mirror analyzer coupled with a quadrupole mass spectrometer. Energy distributions have been measured for oxygen, nitrogen and inert gas ions incident with from 15 to 70 eV reflected from amorphous metal surfaces of several compositions. For ions of lighter atomic mass than the reflecting metal, reflected beams have peaked energy distributions; beams with the peak at 4-32 eV have been measured. The energy and mass dependences of the energy distributions as well as measurements of absolute flux, and angular distribution and divergence are reported. Applications of the neutral beams produced are described.

Author: Ehrlich, K.

Year: 2003

Title: The development of structural materials for fusion reactors

Journal: Materialwissenschaft Und Werkstofftechnik

Volume: 34

Issue: 1

Pages: 39-48

Date: Jan

Accession Number: ISI:000180848400007

Abstract: Structural materials for the First Wall and breeding blankets of future fusion reactors will be exposed to intense neutron irradiation and thermal wall loading. Fusion-specific selection criteria for the proper choice of materials are primary damage parameters, a minimum of produced radioactivity (low activation materials) and also conventional properties like strength and corrosion resistance. Three major material groups are under discussion: ferritic-martensitic 7-12%Cr steels, SiC-fiber-enforced compound materials of type SiCp/SiC and specific vanadium-based alloys. A short status of development and a survey on necessary further research work is given to fulfil the material requirements for the construction of the next fusion reactor devices. Finally the necessity for an appropriate 14 MeV neutron source as test bed for the material development is mentioned.

Author: Evtikhin, V. A.; Lyublinski, I. E.; Pankratov, V. Y.; Zavyalski, L. P.

Year: 1992

Title: Vanadium Alloys as Structural-Materials for Liquid Lithium Blanket of Fusion-Reactors

Journal: Journal of Nuclear Materials

Volume: 191

Pages: 924-927

Date: Sep

Accession Number: ISI:A1992JY94700056

Abstract: The behaviour of V and V-5Ti, V-15Ti-10Cr-0.05Y, V-8Cr-1Zr-0.1C, V-8Cr-5Ti-1Zr-0.1C, V-4Cr-0.5Ti-0.1Zr-0.04Si, V-9Ti-5Cr-0.04Zr-0.04Si alloys was studied. Experiments were conducted under static conditions at 450 and 700-degrees-C for exposure times up to 2600 h. Experiments in dynamic lithium with 400 wppm nitrogen contamination were also conducted in the convection loop at 450-degrees-C for 2600 h Li exposure. Neither significant corrosion nor deterioration of mechanical properties were found after the static lithium tests at 450-degrees-C. Experiments at 700-degrees-C for 1050 h showed that without protective covering V-base alloys cannot be used as blanket structural materials at this temperature. Mass transfer of the V-base materials studied in flowing lithium does not depend on alloy composition; the average dissolution rate is 1.3 mg/(m2 h). It appears that the protective nitride film formed on the sample surfaces, decreases the dissolution rate of the V-base alloys, retards further nitrogen and carbon mass transfer, and thus minimizes the effect of a lithium environment on mechanical properties.

Author: Evtikhin, V. A.; Lyublinski, I. E.; Vertkov, A. V.

Year: 1998

Title: Compatibility of vanadium alloys and its weld joints in homogeneous and heterogeneous liquid lithium systems

Journal: Journal of Nuclear Materials

Volume: 263

Pages: 1487-1491

Date: Oct

Accession Number: ISI:000077203500063

Abstract: The self-cooled liquid lithium fusion reactor blanket concept has considerable attractions. Liquid lithium compatible structure materials working at high temperature and under liquid metal flow conditions are needed for realization of the concept. On the basis of the corrosion tests of vanadium-based alloys and vanadium alloys together with 316Ti type SS, some conclusions and recommendations are given for the optimization of liquid metal blanket operating conditions, alloys composition, lithium purity and material choice. (C) 1998 Elsevier Science B.V. All rights reserved.

Author: Indacochea, J. E.; Smith, J. L.; Litko, K. R.; Karell, E. J.

Year: 1999

Title: Corrosion performance of ferrous and refractory metals in molten salts under reducing conditions

Journal: Journal of Materials Research

Volume: 14

Issue: 5

Pages: 1990-1995

Date: May

Accession Number: ISI:000082550500044

Abstract: A lithium reduction technique to condition spent fuel for disposal has been developed at the Argonne National Laboratory. There is a need to ensure adequate vessel longevity through corrosion testing and, if necessary, materials development. Several ferrous alloys and tantalum specimens were submitted to a corrosion test at 725 degrees C for thirty days in an argon atmosphere, using a lithium-chloride salt saturated with lithium metal and containing small amounts of lithium oxide and lithium nitride. The samples did not show dimensional or weight change, nor could corrosion attack be detected metallographically. The lithium-saturated salt system did not show any behavior similar to that of liquid lithium corrosion. From testing in other gas compositions, it appears that the presence of oxygen in the system is necessary to produce severe corrosion.

Author: Jones, R. H.; Henager, C. H.; Hollenberg, G. W.

Year: 1992

Title: Composite-Materials for Fusion Applications

Journal: Journal of Nuclear Materials

Volume: 191

Pages: 75-83

Date: Sep

Accession Number: ISI:A1992JY41700012

Abstract: Ceramic matrix composites, CMCs, are being considered for advanced first wall and blanket structural applications because of their high-temperature properties, low neutron activation, low density and low coefficient of expansion coupled with good thermal conductivity and corrosion behavior. This paper presents a review and analysis of the hermetic, thermal conductivity, corrosion, crack growth and radiation damage properties of CMCs.

Author: Kalin, B. A.; Fedotov, V. T.; Grigoriev, A. E.; Sevriukov, O. N.; Pliushev, A. N.; Skuratov, L. A.; Polsky, V. I.; Yakushin, V. L.; Virgiliev, Y. S.; Vasiliev, V. L.; Tserevitinov, S. S.

Year: 1995

Title: Application of Amorphous Filler Metals in Production of Fusion-Reactor High Heat-Flux Components

Journal: Fusion Engineering and Design

Volume: 28

Pages: 119-124

Date: Mar

Accession Number: ISI:A1995QU34300016

Abstract: Amorphous ribbon-type filler metals represent a promising facility for fastening heterogeneous materials together. The advantage results from the homogeneity of element and phase compositions and the strictly specified geometrical dimensions of such fillers. Amorphous fillers Zr-Ti-Fe-Be, Zr-Ti-Ni-Cu and Ti-Zr-Ni-Cu and microcrystalline fillers Al-Si and Cu-Sn-Mn-In-Ni were produced by quenching at a rate of about 10(6) K s(-1). Brazing of graphite with metals (Cu + MPG-6, Cu + RGT, Mo + MIG-1, V + MIG-1, V + RGT) was accomplished using ribbon-type fillers. Two types of metal-based samples were produced in the form of plates and rakes. The rakes were made by brazing three small graphite bars to the metal, the 2 mm space between the bars being 0.25 of the bar height. The results of metallographic studies of the brazing zone and of tests on brazed structures treated by pulsed energy fluxes are discussed.

Author: Lucon, E.; van Walle, E.; Decreton, M.

Year: 2001

Title: Mechanical characterization of two low-activation chromium alloys in as-received and heat-treated conditions

Journal: Fusion Technology

Volume: 39

Issue: 2

Pages: 569-573

Date: Mar

Accession Number: ISI:000167919100049

Abstract: In recent years, programmes, attention has been devoted to the characterization of Chromium (Cr) alloys, in view of their elevated corrosion resistance, low activation properties and high-temperature mechanical strength. As part of the European Fusion Programme, an activity has been launched in 1999 with the aim of exploring the potential of Cr alloys as structural materials in fusion reactors, for example, as first wall or blanket materials. Recent investigations have focused attention on two commercially available materials: high-purity 99.7% Cr (DUCROPUR) and Cr alloyed with 5% Fe and 1%Y2O3 (DUCROLLOY), both of which have shown excellent low activation characteristics. The mechanical properties of these two alloys, in both as-received and heat-treated conditions, have been characterized at SCK . CEN by means or tensile, instrumented impact and static three-point bend tests, using standard and sub-size specimens. Tensile tests have also been carried out on samples irradiated at 300 degreesC in the BR2 reactor in Mol up to an accumulated dose of about 0.5 dpa.

Author: Mannheim, R. L.; Garin, J. L.

Year: 2000

Title: Strain hardening of rhenium and two typical molybdenum-rhenium alloys manufactured by powder sintering

Journal: Zeitschrift Fur Metallkunde

Volume: 91

Issue: 10

Pages: 848-853

Date: Oct

Accession Number: ISI:000165530600010

Abstract: Rhenium is a very beneficial alloying addition to form solid solutions with the refractory metals because it greatly enhances the ductility and tensile strength. Among these metals molybdenum is particularly more advantageous because of availability, lower cost and high-temperature strength levels of Mo-Re alloys. The work hardening behavior of Re together with Mo-25Re and Mo-50Re alloys were investigated by cold rolling of powder sintered specimens in the deformation range of 5 to 25 %. The work hardening characteristics of the studied materials were determined by means of the flow curve sigma = K epsilon (n). Both the strain hardening coefficient and the stress at epsilon =1.0 were obtained from a log-log plot based on the experimental data. The n values resulted to be 0.78, 0.45, and 0.70 for pure Re, Mo-25Re and Mo-50Re, respectively, while the corresponding stress factors amounted to 28,718, 4,771 and 8,300MPa. The rapid variations of these values upon increasing the content of Re is a clear proof of the remarkable properties that Re imposes on the base metal.

Author: Marmy, P.; Leguey, T.; Belianov, I.; Victoria, M.

Year: 2000

Title: Tensile and fatigue properties of two titanium alloys as candidate materials for fusion reactors

Journal: Journal of Nuclear Materials

Volume: 283

Pages: 602-606

Date: Dec

Accession Number: ISI:000165877600111

Abstract: Titanium alloys have been identified as candidate structural materials for the first wall, the blanket and the magnetic coil structures of fusion reactors. Titanium alloys are interesting materials because of their high specific strength and low elastic modulus, their low swelling tendency and their fast induced radioactivity decay. Other attractive properties are an excellent resistance to corrosion and good weldability, even in thick sections. Furthermore titanium alloys are suitable for components exposed to heat loads since they have a low thermal stress parameter. Titanium alloys with an a structure are believed to have a good resistance against radiation embrittlement and alpha + beta alloys should possess the best tolerance to hydrogen embrittlement. Two classical industrially available alloys in the two families, the Ti5Al2.4Sn and the Ti6Al4V alloys have been used in this study. The tensile properties between room temperature and 450 degreesC are reported. A low cycle fatigue analysis has been performed under strain control at total strain ranges between 0.8% and 2% and at a temperature of 350 degreesC. The microstructure of both alloys was investigated before and after both types of deformation. Both alloys exhibit excellent mechanical properties comparable to or better than those of ferritic martensitic steels. (C) 2000 Elsevier Science B.V. All rights reserved.

Author: McCarthy, K. A.; Petti, D. A.; Khater, H. Y.

Year: 2001

Title: Comparison of the safety and environmental characteristics of refractory alloys under consideration in APEX

Journal: Fusion Technology

Volume: 39

Issue: 2

Pages: 951-955

Date: Mar

Accession Number: ISI:000167919100115

Abstract: High temperature refractory alloys of tungsten, molybdenum and tantalum are under evaluation for use as structural materials in the Advanced Power Extraction Program (APEX) because of their ability to accommodate high wall loading and high temperature coolant. However, such materials tend to have undesirable safety and environmental characteristics relative to conventional reduced-activation fusion materials. These alloys have high decay heat and in some cases their activation results in the production of long-lived isotopes that would disqualify the material from being disposed of as low level waste. In addition, some of the alloys have oxides that are very volatile, which could be mobilized in accident scenarios in which air ingress is a concern. In this paper we compare the safety and environmental characteristics of these alloys with their low activation cousin (vanadium) in terms of decay heat, oxidation driven mobilization in air, and waste management.

Author: Merker, J.; Fischer, B.; Volkl, R.; Lupton, D. F.

Year: 2003

Title: Investigations of new oxide dispersion hardened platinum materials in laboratory tests and industrial applications

Book Title: Thermec'2003, Pts 1-5

Volume: 426-4

Pages: 1979-1984

Series Title: Materials Science Forum

Accession Number: ISI:000183626400315

Abstract: There is a constantly increasing need for metallic materials with melting points over 1700degreesC for use at very high temperatures. In contrast to the refractory metals: tantalum, niobium, tungsten, molybdenum and rhenium, which also have very high melting points, the platinum materials are characterised by outstanding chemical stability, oxidation resistance and resistance to many molten oxides. Apart from the solid solution hardened alloys, dispersion strengthened platinum materials have also been well-known for a long time. However, these dispersion strengthened platinum materials show considerable problems during the manufacturing process. This paper reports on a new class of oxide dispersion hardened platinum materials (Pt DPH materials). These materials, manufactured by Heraeus, have been the subject of a detailed programme of laboratory investigations and industrial tests. By means of the development of these materials, it is now possible to avoid the disadvantages mentioned above. After a short introduction describing the manufacture and structure of the new DPH materials the report gives comprehensive results on the laboratory and industrial tests. The results of stress-rupture tests and creep tests confirm that the novel DPH materials display high temperature strength, low creep rate and simultaneously very good ductility. The Pt DPH materials also show excellent properties even after welding and corrosion exposure in aggressive glass melts.

Author: Nakamura, H.; Takemura, M.; Yamauchi, M.; Fischer, U.; Ida, M.; Mori, S.; Nishitani, T.; Simakov, S.; Sugimoto, M.

Year: 2005

Title: Accessibility evaluation of the IFMIF liquid lithium loop considering activated erosion/corrosion materials deposition

Journal: Fusion Engineering and Design

Volume: 75-9

Pages: 1169-1172

Date: Nov

Accession Number: ISI:000234072100202

Abstract: This paper presents an evaluation of accessibility of the Li loop piping considering activated corrosion product. International Fusion Materials Irradiation Facility (IFMIF) is a deuteron-lithium (Li) stripping reaction neutron source for fusion materials testing. Target assembly and back wall are designed as fully remote maintenance component. Accessibility around the Li loop piping will depend on activation level of the deposition materials due to the back wall erosion/corrosion process under liquid Li flow. Activation level of the corrosion products coming from the AISI 316LN back wall is calculated by the ACT-4 of the THIDA-2 code system. The total activities after I day, I week, I month and I year cooling are 3.1 X 10(14), 2.8 x 10(14), 2.3 x 10(14) and 7.5 x 10(13) Bq/kg, respectively. Radiation dose rate around the Li loop pipe is calculated by QAD-CGGP2R code. Activated area of the back wall is 100 cm(2). Corrosion rate is assumed I mu m/year. When 10% of the corrosion material is supposed to be deposited on the inner surface of the pipe, the dose rate is calculated to be less than a permissible level of 10 mu Sv/h for hands-on maintenance, therefore, the maintenance work is assessed to be possible. (c) 2005 Elsevier B.V. All rights reserved.

Author: Natesan, K.; Reed, C. B.; Mattas, R. F.

Year: 1995

Title: Assessment of Alkali-Metal Coolants for the Iter Blanket

Journal: Fusion Engineering and Design

Volume: 27

Pages: 457-466

Date: Mar

Accession Number: ISI:A1995QU00600048

Abstract: The blanket system is one of the most important components of a fusion reactor becuase it has a major impact on both the economics and safety of fusion energy. The primary functions of the blanket in a deuterium-tritium-fueled fusion reactor are to convert the fusion energy into sensible heat and to breed tritium for the fuel cycle. The Blanket Comparison and Selection Study, conducted earlier, described the overall comparative performance of various blanket concepts, including liquid metal, molten salt, water, and helium. This paper discusses the International Thermonuclear Experimental Reactor requirements for a self-cooled blanket that uses liquid Li and for indirectly cooled blankets that use other alkali metals such as NaK. The paper addresses the thermodynamics of interactions between the liquid metals (e.g. Li and NaK) and structural materials (e.g. V-base alloys), together with associated corrosion and compatibility issues. Available experimental data are used to assess the long-term performance of the first wall in a liquid metal environment. Other key issues include development of electrically insulating coatings for the first-wall structural material to minimize magnetohydrodynamic (MHD) pressure drop, and tritium permeation and inventory in self-cooled and indirectly cooled blankets. Acceptable types of coating (based on their chemical compatibility and physical properties) are identified, and surface modifications to achieve these coatings on the first wall are discussed. The assessment examines the extent of our knowledge on the performance of structural materials in liquid metals and identifies needed research and development in several areas to establish performance envelopes for the first wall in a liquid metal environment.

Author: Nazarov, E. G.; Rasulev, U. K.; Khudaeva, G. B.

Year: 1995

Title: Comparative studies of thermal emitters made of molybdenum monocrystal

Journal: Russian Metallurgy

Issue: 5

Pages: 123-127

Accession Number: ISI:A1995UH04700021

Abstract: New materials for thermal emitters based on cheap and available molybdenum which combine high ionization efficiency and convenient service of iridium, rhenium and platinum have been developed. Thermal emitters from molybdenum molybdenum monocrystal alloyed with iridium, rhenium, platinum and tungsten allow higher operating temperatures (<900 K) which permits them to be applied in analyzing high-temperature and high-molecular amines and their derivatives. New efficient thermal emitters for surface ionization detectors show better stability and reliability in long-term service at elevated temperature (<900 K).

Author: Nishimura, H.; Terai, T.; Yoneoka, T.; Tanaka, S.; Sagara, A.; Motojima, O.

Year: 2000

Title: Compatibility of structural candidate materials with LiF-BeF2 molten salt mixture

Journal: Journal of Nuclear Materials

Volume: 283

Pages: 1326-1331

Date: Dec

Accession Number: ISI:000165877800122

Abstract: Compatibility of structural materials such as JLF-1 (Fe-9Cr-2W), vanadium alloys (e.g., V-5Cr-5Ti) and SiC with Flibe (LiF-BeF2) is a key issue for the force-free helical reactor (FFHR) blanket concept. Ill the present study, the corrosion behavior of SUS430 (Fe-18Cr) and SiC in static Flibe was investigated as a first step. After being dipped in Flibe containing a trace of HF at 550 degreesC for 1 day, 3 days and 10 days, specimens were analyzed by X-ray diffractometry (XRD) and Rutherford backscattering spectroscopy (RBS). It was found that SUS430 specimens formed an oxide layer on the surface. However, it was not clear whether the SiC specimens were corroded or not due to a thick deposit. (C) 2000 Elsevier Science B.V. All rights reserved.

Author: Nishimura, H.; Suzuki, A.; Terai, T.; Yamawaki, M.; Tanaka, S.; Sagara, A.; Motojima, O.

Year: 2001

Title: Chemical behavior of Li2BeF4 molten salt as a liquid tritium breeder

Journal: Fusion Engineering and Design

Volume: 58-9

Pages: 667-672

Date: Nov

Accession Number: ISI:000172991100113

Abstract: Research results on chemical behavior of Flibe (LiF-BeF2 molten salt) are reviewed, being focused on tritium release and corrosion against structural materials. Tritium release behavior depended on the REDOX potential in the system. The chemical form changed from TF to HT or T-2 with increasing H-2 partial pressure of the purge gas, and tritium release rate increased also with that, which can be explained well by a tritium release model with an isotopic exchange reaction in the salt. As for the corrosion behavior, a thermodynamic analysis and static experiment were carried out. It was suggested that some kinds of oxide layers can work as a protective scale for ferritic steel, while for V-based alloys, no stable oxide film can exist in the presence of Flibe. REDOX control and/or corrosion-resistant coating should be developed for the corrosion problem. It is concluded that the REDOX control is a key issue for Flibe blanket systems, and future R&D items are pointed out. (C) 2001 Elsevier Science B.V. All rights reserved.

Author: Park, J. H.; Cho, W. D.

Year: 1995

Title: Intermetallic and Electrical Insulator Coatings on High-Temperature Alloys, Properties in Liquid-Lithium Environments

Journal: Materials and Manufacturing Processes

Volume: 10

Issue: 5

Pages: 971-986

Accession Number: ISI:A1995RX37500007

Abstract: In the design of liquid-metal cooling systems for fusion-reactor blanket applications, the corrosion resistance of structural materials and the magnetohydrodynamic (MHD) force and its subsequent influence on thermal hydraulics and corrosion are major concerns. When the system is cooled by liquid metals, insulator coatings are required on piping surfaces in contact with the coolant. The objective of this study is to develop stable corrosion-resistant electrical insulator coatings at the liquid-metal/structural-material interface, with emphasis on electrically insulating coatings that prevent adverse MHD-generated currents from passing through the structural wall, and on Be-V intermetallic coatings for first-wall components that face the plasma. Vanadium and V-base alloys (V-Ti or V-Ti-Cr) are leading candidate materials for structural applications in a fusion reactor. Various intermetallic films were produced on V-alloys and on Types 304 and 316 stainless steel. The intermetallic layers were developed by exposure of the materials to liquid Li containing < 5 at.% dissolved metallic solutes (e.g., Al, Be, Si, Pt, and Cr) at temperatures of 416-880 degrees C. In principle, intermetallic layers can be converted to electrically insulating coatings by insitu oxidation or nitration. Oxygen or oxygen/nitrogen-rich surface layers were developed on V-base alloys by exposure to flowing 99.999% pure Ar or N-2 at temperatures of 500-1030 degrees C. CaO electrical insulator coatings were produced by reaction of the oxygen-rich layer with < 5 at.% Ca dissolved in liquid Li at 400-700 degrees C. The reaction converted the oxygen-rich layer to an electrically insulating film. This coating method is applicable to reactor components because the liquid metal can be used over and over; only the solute within the liquid metal is consumed. The technique can be applied to various shapes (e.g., inside/outside of tubes, complex geometrical shapes) because the coating is formed by liquid-phase reaction. This paper will discuss initial results on the nature of the coatings (composition, thickness, adhesion, surface coverage) and their in-situ electrical resistivity characteristics in liquid Li at high temperatures.

Author: Park, J. H.; Domenico, T.; Dragel, G.; Clark, R.

Year: 1995

Title: Development of Electrical Insulator Coatings for Fusion Power Applications

Journal: Fusion Engineering and Design

Volume: 27

Pages: 682-695

Date: Mar

Accession Number: ISI:A1995QU00600073

Abstract: In the design of liquid-metal cooling systems for fusion blanket applications, the corrosion resistance of structural materials and the magnetohydrodynamic (MHD) force and its subsequent influence on thermal hydraulics and corrosion are major concerns. The objective of this study was to develop stable corrosion-resistant electrical insulator coatings at the liquid-metal-structural-material interface, with emphasis on electrically insulating coatings that prevent adverse MHD-generated currents from passing through the structural walls. Vanadium and V-base alloys (V-Ti or V-Ti-Cr) are leading candidate materials for structural applications in fusion reactors. When the system is cooled by liquid metals, insulator coatings are required on piping surfaces in contact with the coolant. Various intermetallic films were produced on V, V-5Ti, and V-20Ti, V-5Cr-5Ti, and V-15Cr-5Ti, and Ti, and on types 304 and 316 stainless steel. The intermetallic layers were developed by exposure of the materials to liquid Li containing 3-5 at.% dissolved metallic solute (e.g. Al, Be, Mg, Si, Ca, Pt, and Cr) at temperatures of 416-880 degrees C. Subsequently, electrical insulator coatings were produced by reaction of the reactive layers with dissolved N in liquid Li or by air oxidation under controlled conditions at 600-1000 degrees C. These reactions converted the intermetallic layers to electrically insulating oxide-nitride or oxynitride layers. This coating method is applicable to reactor components. The liquid metal can be used over and over because only the solutes are consumed within the liquid metal. The technique can be applied to various shapes (e.g. inside or outside of tubes, complex geometrical shapes) because the coating is formed by liquid-phase reaction. This paper discusses initial results on the nature of the coatings (composition, thickness, adhesion, surface coverage) and their in situ electrical resistivity characteristics in liquid Li at high temperatures.

Author: Petti, D. A.; Anderl, R. A.; Smolik, G. R.; Sze, D. K.; Terai, T.; Tanaka, S.

Year: 2002

Title: Jupiter-II Flibe tritium/chemistry and safety experimental program

Journal: Fusion Science and Technology

Volume: 41

Issue: 3

Pages: 807-811

Date: May

Accession Number: ISI:000175564800097

Abstract: The second Japan/US Program on Irradiation Tests for Fusion Research (JUPITER-II) began on April 1, 2001. Part of the collaborative research centers on studies of the molten salt 2LiF-BeF2 (also known as Flibe) for fusion applications. Flibe has been proposed as a self-cooled breeder in both magnetic and inertial fusion power plant designs over the last twenty years. The key feasibility issues associated with the use of Flibe are the corrosion of structural material by the molten salt, tritium control in the molten salt blanket system, and safe handling practices and releases from Flibe during an accidental spill. An overview of the experimental program to address the key feasibility issues is presented.

Author: Petti, D. A.; Smolik, G. R.; Simpson, M. F.; Sharpe, J. P.; Anderl, R. A.; Fukada, S.; Hatano, Y.; Hara, M.; Oya, Y.; Terai, T.; Sze, D. K.; Tanaka, S.

Year: 2006

Title: JUPITER-II molten salt Flibe research: An update on tritium, mobilization and redox chemistry experiments

Journal: Fusion Engineering and Design

Volume: 81

Issue: 8-14

Pages: 1439-1449

Date: Feb

Accession Number: ISI:000235679300083

Abstract: The second Japan/US Program on Irradiation Tests for Fusion Research (JUPITER-II) began on April 1, 2001. Part of the collaborative research centers on studies of the molten salt 2LiF(2)-BeF2, (also known as Flibe) for fusion applications. Flibe has been proposed as a self-cooled breeder in both magnetic and inertial fusion power plant designs over the last 25 years. The key feasibility issues associated with the use of Flibe are the corrosion of structural material by the molten salt, tritium behavior and control in the molten salt blanket system, and safe handling practices and releases from Flibe during an accidental spill. These issues are all being addressed under the JUPITER-II program at the Idaho National Laboratory in the Safety and Tritium Applied Research (STAR) facility. In this paper, we review the program to date in the area of tritiun/deuterium behavior, Flibe mobilization under accident conditions and testing of Be as a redox agent to control corrosion. Future activities planned through the end of the collaboration are also presented. (c) 2005 Elsevier B.V. All rights reserved.

Author: Pint, B. A.; Tortorelli, P. F.; Jankowski, A.; Hayes, J.; Muroga, T.; Suzuki, A.; Yeliseyeva, O. I.; Chernov, V. M.

Year: 2004

Title: Recent progress in the development of electrically insulating coatings for a liquid lithium blanket

Journal: Journal of Nuclear Materials

Volume: 329-33

Pages: 119-124

Date: Aug 1

Accession Number: ISI:000223505000017

Abstract: Electrically insulating coatings on the first wall of magnetic confinement reactors are essential to reduce the magnetohydrodynamic (MHD) force that would otherwise inhibit the flow of the lithium coolant. There are very few candidate materials because Li dissolves most oxides and many carbides and nitrides do not have sufficient electrical resistivity for this application. Based on thermodynamic considerations and testing of bulk ceramics, the most promising materials are Y2O3, Er2O3 and AlN. Coatings of these materials are being fabricated by a variety of processing techniques and their resistivity and microstructure characterized. Electrical resistivity results from Y2O3 coatings as-deposited and after exposure to Li are presented. Self-healing and in situ coatings are being investigated based on CaO from Li-Ca and Er2O3 from Li-Er. Because there are likely to be cracks in any coatings, a dual-layer system with a thin outer layer of vanadium appears to be a more attractive MHD coating system. Published by Elsevier B.V.

Author: Pint, B. A.; Moser, J. L.; Tortorelli, R.

Year: 2006

Title: Liquid metal compatibility issues for test blanket modules

Journal: Fusion Engineering and Design

Volume: 81

Issue: 8-14

Pages: 901-908

Date: Feb

Accession Number: ISI:000235679300006

Abstract: Liquid metal compatibility issues are being investigated for two different test blanket modules involving either Li or Pb-17 at .%Li. A solution to the magnetohydrodynamic (MHD) problem for the V-Li concept may be attainable using multilayer coatings or a flow channel insert with vanadium in contact with the flowing Li instead of a ceramic insulating layer. These strategies rely on the expected excellent compatibility of vanadium alloys which is being further investigated. For systems using Pb-17Li, capsule testing of SiC and various alloys is being conducted. Monolithic SiC specimens exposed for 1000h in Pb-Li at 800 and 1100 degrees C showed no mass change after cleaning and no detectable increase in the Si content of the Pb-Li after the test. In order to investigate the behavior of corrosion resistant aluminide coatings, initial capsule testing at 700 degrees C has been used to establish baseline dissolution rates for 316 stainless steel, FeCrAl, Fe3Al and NiAl. The samples containing Al showed significantly less mass loss than 316 stainless steel, suggesting that aluminide coatings will be beneficial in this temperature range. (c) 2005 Elsevier B.V. All rights reserved.

Author: Sakurai, T.; Yoneoka, T.; Tanaka, S.; Suzuki, A.; Muroga, T.

Year: 2001

Title: Compatibility test of SiC/SiC composite materials and AlN with liquid Li and Li17Pb83

Journal: Fusion Technology

Volume: 39

Issue: 2

Pages: 649-653

Date: Mar

Accession Number: ISI:000167919100064

Abstract: A purpose of the present study is to investigate the compatibility of SiC/SiC composite material and AIN ceramics with Liquid metals. Corrosion behavior of materials could be affected by non-metallic impurities like nitrogen in liquid lithium. Another purpose of the present study is to control the concentration of nitrogen impurity by using getter materials and to study the effect of getter materials on compatibility with AlN. At 700K, all of the SiC/SiC specimens, except high purity specimen, were entirely broken down in liquid lithium. Even in this high purity specimen, many cracks were observed on the surface. On the other hand, in the case of SiC/SiC with Li17Pb83 at 773K, all of the specimens were not corroded. At 673K, impurity levels in AlN were changed in the case immersed in liquid lithium with getter materials. At 823K, impurities in AW were attacked by lithium and the surface of it was locally peeled off. It was also observed that the getter material captured nitrogen.

Author: Smid, I.; Croessmann, C. D.; Salmonson, J. C.; Whitley, J. B.; Kny, E.; Reheis, N.; Kneringer, G.; Nickel, H.

Year: 1991

Title: Brazed Graphite Refractory-Metal Composites for 1st-Wall Protection Elements

Journal: Journal of Nuclear Materials

Volume: 179

Pages: 169-172

Date: Mar-Apr

Accession Number: ISI:A1991FR77000029

Abstract: The peak surface heat flux deposition on divertor elements of near term fusion devices is expected to exceed 10 MW/m2. The needed reliability of brazed plasma interactive components, particularly under abnormal operating conditions with peak surface temperatures well beyond 1000-degrees-C, makes refractory metallic substrates and brazes with a high melting point very attractive. TZM, a high temperature alloy of molybdenum, and isotropic graphite, materials very closely matched in their thermal expansion, were brazed with four high-temperature brazes. The brazes used were Zr, 90Ni/10Ti, 90Cu/10Ti and 70Ag/27Cu/3Ti (nominal composition prior to brazing, wt%). The resulting composite tiles of 50 x 50 mm2 with a TZM thickness of 5 mm and a graphite thickness of 10 mm have been tested in high heat flux simulation for their thermal fatigue properties. Up to 600 loading cycles were carried out with an average heat flux of 10 MW/m2 for 0.5 s pulses. The maximum surface temperature was 1100-degrees-C. In support of the experiment, the thermal response and temperature gradients of the samples were investigated using a finite element model.

Author: Smith, D. L.; Billone, M. C.; Natesan, K.

Year: 2000

Title: Vanadium-base alloys for fusion first-wall/blanket applications

Journal: International Journal of Refractory Metals & Hard Materials

Volume: 18

Issue: 4-5

Pages: 213-224

Accession Number: ISI:000166627900004

Abstract: Vanadium alloys have been identified as a leading candidate material for fusion first-wall/blanket applications. Certain vanadium alloys exhibit favorable safety and environmental characteristics. good fabricability high temperature and heat load capability, good compatibility with liquid metal coolants and resistance to irradiation damage. The current focus is on vanadium alloys with (3-9 wt%) Cr and (3-10 wt%) Ti with a V-4Cr 4Ti alloy as the reference composition. Substantial progress has been made in the development of vanadium alloys for the fusion first wall/blanket applications including production and welding, characterization of baseline properties, corrosion/compatibility. and effects of irradiation on the properties. This paper presents an overview of the development of vanadium alloys for fusion applications and a summary of key issues requiring further research. (C) 2001 Published by Elsevier Science Ltd.

Author: Suzuki, A.; Muroga, T.; Pint, B. A.; Yoneoka, T.; Tanaka, S.

Year: 2003

Title: Corrosion behaviour of AlN for self-cooled Li/V blanket application

Journal: Fusion Engineering and Design

Volume: 69

Issue: 1-4

Pages: 397-401

Date: Sep

Accession Number: ISI:000185638700068

Abstract: Corrosion behaviour of Aluminum nitride (AlN) as a candidate material for insulating coating for V/Li blanket was investigated by corrosion experiments in liquid lithium (Li) up to 1073 K for 1000 h. High purity AlN samples decreased their weights after the sintering test in Li in contact with vanadium alloy over 973 K, while those in Li not in contact with the vanadium alloy survived up to 1073 K. Nitrogen dissolution from AlN into the liquid Li and absorption of dissolved nitrogen by vanadium alloy are considered to be a corrosion mechanism. Small decreases of electrical resistance were observed after the sintering tests over 873 K because of the conductive corrosion layer on the surface caused by the nitrogen dissolution. In the cases of low purity AlN samples sintered over 973 K, large weight decreases were explained by fragile grain boundary caused by oxygen dissolution. The oxygen dissolution may also results in the resistivity decrease even at 723 K. Therefore, decrease of oxygen impurity in AlN and addition of nitrogen in liquid Li are considered to give a possible solution to the Li/AlN corrosion problem in the Li/AlN/V alloy blanket system. (C) 2003 Elsevier Science B.V. All rights reserved.

Author: Suzuki, A.; Muroga, T.; Yoneoka, T.; Tanaka, S.

Year: 2005

Title: Compatibility of compound oxides with liquid lithium for fusion reactor blanket application

Journal: Journal of Physics and Chemistry of Solids

Volume: 66

Issue: 2-4

Pages: 690-693

Date: Feb-Apr

Accession Number: ISI:000227576500094

Abstract: Mixed oxide phases as candidates for a magnethydrodymanics (MHD) coating material in liquid lithium blanket concept were investigated by immersing in liquid lithium. CaZrO3 showed a better compatibility than MgTiO3, MgZrO3 and CaTiO3 with respect to mass and thickness changes and electrical resistance. With increasing density of CaZrO3 sample, better compatibility at 823 K was observed. In case of a low density sample, Li introduced inside of the sample through the opening channel removed the grains itself to increase the corrosion rate to 30 mu m/year, while the rate was 11 mu m/year in case of high-density sample. CaZrO3 samples containing excess of ZrO2 Showed significant decrease of their compatibility at 673 K, for the micro ZrO2 phase, which is unstable in lithium, may he corroded selectively. Thus, the fabrication of high-density coating with Ca to Zr composition ratio being I to I is considered to be the key ingredient for the corrosion-resistance. (c) 2005 Elsevier Ltd. All rights reserved.

Author: Sviatoslavskya, I. N.; Sawan, M. E.; Mogahed, E. A.; Majumdar, S.; Mattas, R.; Malang, S.; Fogarty, P. J.; Friend, M.; Wong, C. P. C.; Sharafat, S.

Year: 2004

Title: Engineering and geometric aspects of the solid wall re-circulating fluid blanket based on advanced ferritic steel

Journal: Fusion Engineering and Design

Volume: 72

Issue: 1-3

Pages: 307-326

Date: Nov

Accession Number: ISI:000225142500016

Abstract: The Advanced Power Extraction (APEX) project has been exploring concepts for power producing blankets that can enhance the potential of fusion energy. The pursued concepts cover both liquid and solid wall designs. The solid wall blanket branch of the project has been concentrating on the use of nano-composited ferritic (NCF) steel structure coupled with Flibe (Li2BeF4) coolant. The present blanket is a solid wall design with an innovative coolant scheme, which allows part of the coolant to be re-circulated in order to enhance the outlet temperature, and thus improve the power cycle efficiency. The structure is 12YWT, an oxide dispersion strengthened (ODS) ferritic steel, which has a maximum operating temperature of 800 degreesC and a compatibility with Flibe up to 700 degreesC. Several methods for fabricating the complex geometry of the first wall (FW) and blanket are presented. Preliminary coolant routing is proposed with solutions offered for minimizing heat losses and simplifying assembly and maintenance. Even though this blanket is somewhat complicated, its forward looking aims, that of maximizing nuclear performance to achieve a high thermal conversion efficiency, are well worth striving for. (C) 2004 Elsevier B.V. All rights reserved.

Author: Terai, T.; Hosoya, Y.; Tanaka, S.; Sagara, A.; Motojima, O.

Year: 1998

Title: Compatibility of structural materials with Li2BeF4 molten salt breeder

Journal: Journal of Nuclear Materials

Volume: 263

Pages: 513-518

Date: Oct

Accession Number: ISI:000077277000073

Abstract: Compatibility of structural materials (ferritic steel, vanadium-based alloy and molybdenum) with molten LiF-BeF2 mixture under the atmosphere containing O-2, H2O and HF was studied using thermodynamical calculation of chemical equilibria at 823 K. It was clarified that the oxidation of structural materials would have precedence over fluorination with coexistence of oxidizing species though fluorination was found under the atmosphere containing HF. Then, these materials would have satisfactory corrosion resistance if generated oxides function as protective scales. (C) 1998 Elsevier Science B.V. All rights reserved.

Author: Terai, T.; Suzuki, A.; Yoneoka, T.; Mitsuyama, T.

Year: 2000

Title: Compatibility of AlN with liquid lithium

Journal: Journal of Nuclear Materials

Volume: 283

Pages: 1322-1325

Date: Dec

Accession Number: ISI:000165877800121

Abstract: Development of ceramic coatings is one of the most important subjects in liquid blanket research and development. Compatibility of sintered AIN and AIN coatings with liquid lithium, a candidate breeding material, was investigated. Sintered AIN with or without the sintering aid of Y2O3 examined in lithium at 773 K for 1390 h showed a slight decrease in electrical resistivity because of a reduction in Al2O3 impurity, though AIN and Y2O3 components themselves were subject to no severe corrosion. On the other hand, AIN ceramic coatings on SUS430 with high resistivity (>10(11) Omega m) fabricated by the RF sputtering method disappeared in liquid lithium at 773 K in 56 h. This may be because cracks were formed due to the difference in thermal expansion between the coatings and the substrate or because the oxide formed between the two was removed by liquid lithium. (C) 2000 Elsevier Science B.V. All rights reserved.

Author: Terai, T.; Nishimura, H.; Yamaguchi, K.; Yamawaki, M.; Suzuki, A.; Muroga, T.; Sagara, A.; Motojima, O.

Year: 2001

Title: Compatibility of structural materials with Li2BeF4 molten salt breeder

Journal: Fusion Technology

Volume: 39

Issue: 2

Pages: 784-788

Date: Mar

Accession Number: ISI:000167919100086

Abstract: Research results an corrosion behavior of Flibe (LiF-BeF2 molten salt) against structural materials are reviewed. Thermodynamic calculation and static experiment were carried out. It was found that some kinds of oxide films may work as a protective scale for ferritic steel. For V-based alloy, on the other hand, no stable oxide film can exist in the presence of Flibe. It was also found that Redox control might protect V-based alloy against corrosion.

Author: Votinov, S. N.; Solonin, M. I.; Kazennov, Y. I.; Kondratjev, V. P.; Nikulin, A. D.; Tebus, V. N.; Adamov, E. O.; Bougaenko, S. E.; Strebkov, Y. S.; Sidorenkov, A. V.; Ivanov, V. B.; Kazakov, V. A.; Evtikhin, V. A.; Lyublinski, I. E.; Trojanov, V. M.; Rusanov, A. E.; Chernov, V. M.; Birgevoj, G. A.

Year: 1996

Title: Prospects and problems using vanadium alloys as a structural material of the first wall and blanket of fusion reactors

Journal: Journal of Nuclear Materials

Volume: 237

Pages: 370-375

Date: Oct

Accession Number: ISI:A1996WB60300063

Abstract: Vanadium-based alloys are most promising as low activation structural materials for DEMO. It was previously established that high priority is to be given to V-alloys of the V-Ti-Cr system as structural materials of a tritium breeding blanket and the first wall of a fusion reactor. However, there is some uncertainty in selecting a specific element ratio between the alloy components in this system, This is primarily explained by the fact that the properties of V-alloys are dictated not only by the ratio between the main alloying elements (here Ti and Cr), but also by impurities, both metallic and oxygen interstitials. Based on a number of papers today one can say that V-Ti-Cr alloys with insignificant variations in the contents of the main constituents within 5-10 mass% Ti and 4-6 mass% Cr must be taken as a base for subsequent optimization of chemical composition and thermomechanical working. However, the database is obviously insufficient to assess the ecological acceptability (activation), physical and mechanical properties, corrosion and irradiation resistance and, particularly, the commercial production of alloys. Therefore, there is a need for comprehensive studies of promising V-alloys, namely V-4Ti-4Cr and V-10Ti-SCr.

Author: Wall, R. N.; Basch, D. R.; Jacobson, D. L.

Year: 1992

Title: High-Temperature Spectral Emissivity of Several Refractory Elements and Alloys

Journal: Journal of Materials Engineering and Performance

Volume: 1

Issue: 5

Pages: 679-684

Date: Oct

Accession Number: ISI:A1992KG49000008

Abstract: Thermionic energy conversion has emerged as the method of choice for the direct space-based conversion of heat to electricity. An important parameter in the implementation of this method of direct energy conversion is the emissivity of the converter emitter and collector materials. This information is necessary to determine heat losses, heat transfer, and reservoir temperatures in the thermionic energy converter. Spectral normal emissivities were acquired at a wavelength of 0.65 mum for a series of tungsten-rhenium alloys, tungsten-osmium alloys, and tungsten-iridium alloys in the temperature range 1400 to 2600 K. Additionally, the spectral normal emissivity for pure elements of molybdenum and ruthenium were obtained over the temperature range 1200 to 2600 K and 1400 to 2250 K, respectively. The spectral normal emissivities for a niobium-67% ruthenium (eutectic composition) in the temperature range 1400 to 2000 K were also obtained at the same wavelength. In all cases, the emissivity decreased linearly with increasing temperature. Both the tungsten-osmium and the tungsten-rhenium alloys exhibited emissivity values of 0.32 to 0.54 over the temperatures tested. The tungsten-iridium alloy yielded emissivity data of 0.35 to 0.47. The niobium-ruthenium emissivity data were within 0.34 and 0.36. The pure molybdenum and pure ruthenium experiments resulted in emissivity values ranging from 0.35 to 0.45 and 0.35 to 0.39, respectively.

Author: Yamazaki, S.; Miura, H.; Koike, H.; Seki, Y.; Kunugi, T.; Nishio, S.; Aoki, I.; Shimizu, A.

Year: 1994

Title: Design Study of Helium Solid Suspension Cooled Blanket and Divertor Plate for a Tokamak Power-Reactor

Journal: Fusion Engineering and Design

Volume: 25

Issue: 1-3

Pages: 227-238

Date: Aug

Accession Number: ISI:A1994PC63300021

Abstract: High temperature helium gas will provide a thermal efficiency greater than 40%, even using a conventional steam turbine. In addition, helium gas will not react chemically with blanket materials, and surrounding air and water. Tritium will be easily extracted from the coolant too. Thus, it is one of the most attractive coolants for a fusion power reactor, from the economical, safety and environmental points of view. However, a large volumetric flow rate is required owing to the small heat capacity when the pressure is not extremely high. This requires a larger reactor size, larger circulating power and more penetrations, which may increase radiation streaming. A relatively low heat transfer coefficient makes it difficult to apply to a component subjected to a high heat load, such as a divertor plate. We suggest in this study, a helium-solid suspension flow as coolant, to increase the heat capacity and heat transfer coefficient. A gas pressure of 5 MPa, and inlet and outlet temperatures of 400-degrees-C and 700-degrees-C were chosen. There are few candidates for the structural material which can be used at temperatures higher than 900-degrees-C. We have proposed an intermetallic compound of titanium aluminide (TiAl) as candidate structural material of the blanket. Although the database for TiAl is incomplete, it has high strength and ductility at the operation temperature. Using TiAl, radioactive waste management will be mitigated, since its activity will decrease rapidly. The elongation at room temperature, which is only a few per cent, will be improved through,research and development not only in fusion but also in other industrial fields. In this study, spherical pebbles of lithium oxide and small blocks of beryllium were chosen as the breeder and neutron multiplier. Manganese blocks were installed to enhance energy multiplication. A tritium breeding ratio of 1.38 and energy multiplication ratio of 1.35 were obtained with the blanket. The net plant efficiency exceeds 40%, including the circulating power. The peak surface heat flux on the divertor plate was decreased with gas puffing including an

impurity near the striking point. In spite of this, the expected peak heat flux was still several MW m-2 from the result of numerical calculation of the edge plasma. To remove so high a heat load, an impinging helium-solid suspension jet was applied to the high heat flux region of the divertor plate. Molybdenum alloy was used as the structural material in this region to keep the surface temperature and thermal stress lower than the design limits. TiAl was used as the structural material of other regions in the divertor chamber. To prevent excessive sputtering erosion, the electron temperature in the divertor plasma must be kept lower than 20 eV.

Author: Yavlinskii, Y.

Year: 1998

Title: Track formation in amorphous metals under swift heavy ion bombardment

Journal: Nuclear Instruments & Methods in Physics Research Section B-Beam Interactions with Materials and Atoms

Volume: 146

Issue: 1-4

Pages: 142-146

Date: Dec

Accession Number: ISI:000077719400024

Abstract: Recently tracks were observed in amorphous metals irradiated by swift multicharged ion (MCI). The experiment is especially interesting because the track was not revealed if amorphous metal target had been annealed preliminarily. The present paper is devoted to interpretation of the experimental data in terms of the so-called "plasma model". The slowing down of MCI in solids results from the energy loss mainly due to inelastic collisions. Practically almost all energy inputs by projectile are concentrated in excited electrons resulting from ionization processes. The relaxation of the excited electrons happens due to electron-electronic (electronic heat conductivity) and electron-lattice collisions. The cooling time of the excited electron subsystem itself in metals is some orders of magnitude smaller than the typical time of energy transfer from electrons to the lattice which is depended essentially on crystal structure of the target. The rate of electron energy transfer to target atoms is determined by the presence (in single crystals) or the absence (in amorphous metals) of the lattice periodic potential. The melting track should be observed in amorphous target with metallic conductivity, as here the rate of electron energy transfer is more than in single crystal. Crystallisation happens upon annealing, amorphous metal turn into crystal with periodic potential and tracks are not formed. The calculations of final lattice temperature taking into account the increase of melting point at local fusion and lattice thermal conductivity are carried out. (C) 1998 Elsevier Science B.V. All rights reserved.

Author: Yoneoka, T.; Tanaka, S.; Terai, T.

Year: 2001

Title: Compatibility of SiC/SiC composite materials with molten lithium metal and Li16-Pb84 eutectic alloy

Journal: Materials Transactions

Volume: 42

Issue: 6

Pages: 1019-1023

Date: Jun

Accession Number: ISI:000169993000017

Abstract: SiC/SiC composite material is one of the candidates of plasma facing and structural materials for a fusion reactor. In an inertial fusion reactor and a magnetic confinement fusion reactor, interactions of solid and liquid breeder materials as well as coolant materials with various structural materials are considered to be very important. Therefore, corrosion tests of SiC/SiC composite materials with molten lithium and Li16-Pb84 alloy were performed. SiC/SiC specimens of five kinds, different in fiber/matrix interface, manufacturers and manufacturing methods, were used. In the case of lithium, the corrosion temperature was 500 K, and it was 573 K in the case of Li16-Pb84 alloy. Duration for the compatibility tests were about 2.5 Ms (29 days). During the heating of corrosion test, argon gas was made to flow over the liquid metal. The SiC/SiC composite sample, which had a free silicon component within its matrix, was corroded by molten lithium and came to each plane fabrics of fiber. The monolithic specimen that contained a silicon phase was also entirely broken by lithium. While, the attack by Li16-Pb84 alloy was not observed.

Author: Zinkle, S. J.; Ghoniem, N. M.

Year: 2000

Title: Operating temperature windows for fusion reactor structural materials

Journal: Fusion Engineering and Design

Volume: 51-2

Pages: 55-71

Date: Nov

Accession Number: ISI:000165996400005

Abstract: A critical analysis is presented of the operating temperature windows for nine candidate fusion reactor structural materials: four reduced-activation structural materials (oxide-dispersion-strengthened and ferritic/martensitic steels containing 8-12%Cr, V-4Cr-4Ti, and SiC/SiC composites), copper-base alloys (CuNiBe), tantalum-base alloys (e.g. Ta-8W-2Hf), niobium alloys (Nb-1Zr), and molybdenum and tungsten alloys. The results are compared with the operating temperature limits for Type 316 austenitic stainless steel. Several factors define the allowable operating temperature window for structural alloys in a fusion reactor. The lower operating temperature limit in all body-centered cubic (BCC) and most face-centered cubic (FCC) alloys is determined by radiation embrittlement (decrease in fracture toughness), which is generally most pronounced for irradiation temperatures below similar to 0.3 T-M where T-M is the melting temperature. The lower operating temperature limit for SiC/SiC composites will likely be determined by radiation-induced thermal conductivity degradation, which becomes more pronounced in ceramics with decreasing temperature. The upper operating temperature limit of structural materials is determined by one of four factors, all of which become more pronounced with increasing exposure time: (1) thermal creep (grain boundary sliding or matrix diffusional creep); (2) high temperature He embrittlement of grain boundaries; (3) cavity swelling (particularly important for SiC and Cu alloys); or (4) coolant compatibility/corrosion issues. In many cases, the upper temperature limit will be determined by coolant corrosion/compatibility rather than by thermal creep or radiation effects. The compatibility of the structural materials with Li, Pb-Li, Sn-Li, He and Flibe (Li_2BeF_4) coolants is summarized. (C) 2000 Elsevier Science B.V. All rights reserved.